54. Swanson CM, Sherer NM, Malim MH (2010) SRp40 and SRp55 promote the translation of unspliced human immunodeficiency virus type 1 RNA. J Virol 84: 6748–6759.
55. Li N, Flynt AS, Kim HR, Solnica-Krezel L, Patton JG (2008) Dispatched Homolog 2 is targeted by miR-214 through a combination of three weak microRNA recognition sites. Nucleic Acids Res 36: 4277–4285.
56. Hafner M, Landthaler M, Burger L, Khorshid M, Hausser J, et al. (2010) Transcriptome-wide identification of RNA-binding protein and microRNA target sites by PAR-CLIP. Cell 141: 129–141.
57. Schnall-Levin M, Zhao Y, Perrimon N, Berger B (2010) Conserved microRNA targeting in Drosophila is as widespread in coding regions as in 3'UTRs. Proc Natl Acad Sci U S A 107: 15751–15756.
58. Castelló A, Franco D, Moral-López P, Berlanga JJ, Alvarez E, et al. (2009) HIV-1 protease inhibits Cap- and poly(A)-dependent translation upon eIF4GI and PABP cleavage. PLoS One 4: e7997.
59. Charnay N, Ivanyi-Nagy R, Soto-Rifo R, Ohlmann T, López-Lastra M, et al. (2009) Mechanism of HIV-1 Tat RNA translation and its activation by the Tat protein. Retrovirology 6: 74.
60. Romani B, Engelbrecht S (2009) Human immunodeficiency virus type 1 Vpr: functions and molecular interactions. J Gen Virol 90: 1795–1805.
61. Kiriakidou M, Tan GS, Lamprinaki S, De Planell-Saguer M, Nelson PT, et al. (2007) An mRNA m7G cap binding-like motif within human Ago2 represses translation. Cell 129: 1141–1151.
62. Sharma A, Yilmaz A, Marsh K, Cochrane A, Boris-Lawrie K (2012) Thriving under stress: selective translation of HIV-1 structural protein mRNA during Vpr-mediated impairment of eIF4E translation activity. PLoS Pathog 8: e1002612.
63. Ajamian L, Abrahamyan L, Milev M, Ivanov PV, Kulozik AE, et al. (2008) Unexpected roles for UPF1 in HIV-1 RNA metabolism and translation. RNA 14: 914–927.
64. Burdick R, Smith JL, Chaipan C, Friew Y, Chen J, et al. (2010) P body-associated protein Mov10 inhibits HIV-1 replication at multiple stages. J Virol 84: 10241–10253.
65. Furtak V, Mulky A, Rawlings SA, Kozhaya L, Lee K, et al. (2010) Perturbation of the P-body component Mov10 inhibits HIV-1 infectivity. PLoS One 5: e9081.
66. Gallois-Montbrun S, Kramer B, Swanson CM, Byers H, Lynham S, et al. (2007) Antiviral protein APOBEC3G localizes to ribonucleoprotein complexes found in P bodies and stress granules. J Virol 81: 2165–2178.
67. Beckham CJ, Parker R (2008) P bodies, stress granules, and viral life cycles. Cell Host Microbe 3: 206–212.
68. Swanson CM, Malim MH (2006) Retrovirus RNA trafficking: from chromatin to invasive genomes. Traffic 7: 1440–1450.
69. Alce TM, Popik W (2004) APOBEC3G is incorporated into virus-like particles by a direct interaction with HIV-1 Gag nucleocapsid protein. J Biol Chem 279: 34083–34086.
70. Chable-Bessia C, Meziane O, Latreille D, Triboulet R, Zamborlini A, et al. (2009) Suppression of HIV-1 replication by microRNA effectors. Retrovirology 6: 26.
71. Liu J, Valencia-Sanchez MA, Hannon GJ, Parker R (2005) MicroRNA-dependent localization of targeted mRNAs to mammalian P-bodies. Nat Cell Biol 7: 719–723.
72. Huang J, Liang Z, Yang B, Tian H, Ma J, et al. (2007) Derepression of microRNA-mediated protein translation inhibition by apolipoprotein B mRNA-editing enzyme catalytic polypeptide-like 3G (APOBEC3G) and its family members. J Biol Chem 282: 33632–33640.
73. Cullen BR (2010) Five questions about viruses and microRNAs. PLoS Pathog 6: e1000787.
74. Camus G, Segura-Morales C, Molle D, Lopez-Vergès S, Begon-Pescia C, et al. (2007) The clathrin adaptor complex AP-1 binds HIV-1 and MLV Gag and facilitates their budding. Mol Biol Cell 18: 3193–3203.
75. Dong X, Li H, Derdowski A, Ding L, Burnett A, et al. (2005) AP-3 directs the intracellular trafficking of HIV-1 Gag and plays a key role in particle assembly. Cell 120: 663–674.
76. Nydegger S, Foti M, Derdowski A, Spearman P, Thali M (2003) HIV-1 egress is gated through late endosomal membranes. Traffic 4: 902–910.
77. Sherer NM, Lehmann MJ, Jimenez-Soto LF, Ingmundson A, Horner SM, et al. (2003) Visualization of retroviral replication in living cells reveals budding into multivesicular bodies. Traffic 4: 785–801.
78. Tang Y, Leao IC, Coleman EM, Broughton RS, Hildreth JE (2009) Deficiency of niemann-pick type C-1 protein impairs release of human immunodeficiency virus type 1 and results in Gag accumulation in late endosomal/lysosomal compartments. J Virol 83: 7982–7995.
79. Perlman M, Resh MD (2006) Identification of an intracellular trafficking and assembly pathway for HIV-1 gag. Traffic 7: 731–745.
80. Basyuk E, Galli T, Mougel M, Blanchard JM, Sitbon M, et al. (2003) Retroviral genomic RNAs are transported to the plasma membrane by endosomal vesicles. Dev Cell 5: 161–174.
81. Dorweiler IJ, Ruone SJ, Wang H, Burry RW, Mansky LM (2006) Role of the human T-cell leukemia virus type 1 PTAP motif in Gag targeting and particle release. J Virol 80: 3634–3643.
82. Murray JL, Mavrakis M, McDonald NJ, Yilla M, Sheng J, et al. (2005) Rab9 GTPase is required for replication of human immunodeficiency virus type 1, filoviruses, and measles virus. J Virol 79: 11742–11751.
83. Mertz JA, Lozano MM, Dudley JP (2009) Rev and Rex proteins of human complex retroviruses function with the MMTV Rem-responsive element. Retrovirology 6: 10.
84. Anderson EC, Lever AM (2006) Human immunodeficiency virus type 1 Gag polyprotein modulates its own translation. J Virol 80: 10478–1086.
85. Urcuqui-Inchima S, Patiño C, Zapata X, García MP, Arteaga J, et al. (2011) Production of HIV particles is regulated by altering sub-cellular localization and dynamics of Rev induced by double-strand RNA binding protein. PLoS One 6: e16686.
86. Suzuki J, Miyano-Kurosaki N, Kuwasaki T, Takeuchi H, Kawai G, et al. (2002) Inhibition of human immunodeficiency virus type 1 activity in vitro by a new self-stabilized oligonucleotide with guanosine-thymidine quadruplex motifs. J Virol 76: 3015–3022.
87. Komano J, Miyauchi K, Matsuda Z, Yamamoto N (2004) Inhibiting the Arp2/3 complex limits infection of both intracellular mature vaccinia virus and primate lentiviruses. Mol Biol Cell 15: 5197–5207.
88. Sugiyama R, Hayafune M, Habu Y, Yamamoto N, Takaku H (2011) HIV-1 RT-dependent DNAzyme expression inhibits HIV-1 replication without the emergence of escape viruses. Nucleic Acids Res 39: 589–598.
89. Hwang HW, Wentzel EA, Mendell JT (2007) A hexanucleotide element directs microRNA nuclear import. Science 315: 97–100.
90. Schmittgen TD, Livak KJ (2008) Analyzing real-time PCR data by the comparative C(T) method. Nat Protoc 3: 1101–1108.
91. Wang WX, Wilfred BR, Hu Y, Stromberg AJ, Nelson PT (2010) Anti-Argonaute RIP-Chip shows that miRNA transfections alter global patterns of mRNA recruitment to microribonucleoprotein complexes. RNA 16: 394–404.

FEBS Letters 586 (2012) 3562–3568

ELSEVIER

FEBS Letters

journal homepage: www.FEBSLetters.org

ZBRK1 represses HIV-1 LTR-mediated transcription

Hironori Nishitsuji *, Makoto Abe, Reila Sawada, Hiroshi Takaku *

Department of Life and Environmental Sciences, Chiba Institute of Technology, 2-17-1 Tsudanuma, Narashino, Chiba 275-0016, Japan

ARTICLE INFO

Article history:
Received 23 February 2012
Revised 5 August 2012
Accepted 8 August 2012
Available online 17 August 2012

Edited by Ivan Sadowski

Keywords:
KRAB domain
TRIM28
LTR
HIV-1
Zinc finger protein

ABSTRACT

The identification of cellular proteins that interact with the human immunodeficiency virus type 1 (HIV-1) long terminal repeat (LTR) provides a basic understanding of HIV-1 gene expression, which is the major determinant regulating virus replication. We show that ZBRK1 negatively regulates the HIV-1 LTR. Ectopic expression of ZBRK1 represses transcriptional activity of the HIV-1 LTR, whereas the depletion of endogenous ZBRK1 leads to activation of the HIV-1 LTR. The repressor activity of ZBRK1 is required for TRIM28 binding. Furthermore, ZBRK1 is bound to the HIV-1 LTR in vivo. These results indicate that ZBRK1 could be involved in a potent intrinsic antiretroviral defense.

Structured summary of protein interactions:
ZBRK1 physically interacts with **TRIM28** by anti tag coimmunoprecipitation (View interaction).

1. Introduction

The binding of host factors to long terminal repeats (LTRs) of proviral DNA tightly regulates retroviral gene expression. Recent reports have shown that TRIM28 (tripartite motif-containing protein 28; also known as KRAB-associated protein 1 (KAP1)), a well-characterized transcriptional repressor, suppresses endogenous retroviruses by recruiting the H3K9 methyltransferases ESET (also called SETDB1 or KMT1E) and heterochromatin protein 1 (HP1) in mouse ES cells [1–2]. Exogenous retroviruses, such as moloney murine leukemia virus (M-MLV), are also silenced by TRIM28 in ES cells [3]. TRIM28-mediated gene-specific transcriptional repression requires a Krüppel-associated box (KRAB)-zinc finger protein, such as ZFP809, to directly recognize integrated viral DNA [4]. Allouch et al. have proposed that TRIM28 inhibits HIV-1 replication by suppressing IN acetylation during integration [5].

KRAB-zinc finger proteins have the potential to regulate HIV-1 gene expression. Several groups have reported that artificially engineered KRAB domain-containing zinc finger proteins that bind to HIV-1 sequences also induce proviral silencing [6,7]. By contrast, endogenous OTK18, which contains 13 C_2H_2-type zinc finger motifs and a KRAB domain and was identified by differential display of mRNA from HIV type 1-infected macrophages, was shown to interact with and suppress the NRE within the HIV-1 LTR [8]. Thus, some KRAB-zinc finger proteins efficiently inhibit HIV-1 replication.

ZBRK1, which is also known as KRAB-zinc finger protein, binds to the GGGxxxCAGxxxTTT DNA recognition motif within intron 3 of the DNA damage-responsive gene *GADD45* following cellular DNA damage. Previously, breast cancer susceptibility gene1 (BRCA1), which has been shown to interact physiologically with ZBRK1 [9], was identified through large-scale screening as a host factor for HIV-1 replication [10].

ZBRK1 has been implicated in the tumorigenesis of several human cancers. BRCA1, CtIP, and ZBRK1 form a repressor complex at a ZBRK1 recognition site within the *ANG1* promoter, and a defect in the formation of this repressor complex de-represses ANG1 expression. This complex promotes the survival of neighboring endothelial cells [11]. Moreover, ZBRK1 and the ATXN2 complex regulate *SCA2* gene transcription and have been linked to cellular RNA metabolism and endocytotic processes.

We report here the molecular characterization of ZBRK1-mediated HIV-1 LTR repression. ZBRK1 acts as a transcriptional repressor of the HIV-1 LTR in a TRIM28-dependent manner. These data shed further light on the mechanistic role of ZBRK1 in HIV-1 gene expression.

2. Materials and methods

2.1. Plasmids

The details of the plasmid constructs used in this study are provided in the Supplementary Materials and methods section.

2.2. Preparation of lentiviral vectors

293T cells (1×10^6) were plated in 60-mm dishes and co-transfected with the appropriate lentiviral-shRNA expression

* Corresponding authors. Fax: +81 47 478 0407.
E-mail addresses: hironori.nishitsuji@it-chiba.ac.jp (H. Nishitsuji), hiroshi.takaku@it-chiba.ac.jp (H. Takaku).

0014-5793/$36.00 © 2012 Federation of European Biochemical Societies. Published by Elsevier B.V. All rights reserved.
http://dx.doi.org/10.1016/j.febslet.2012.08.010

vector (1.6 μg), the vesicular stomatitis virus G expression vector pMD.G (0.5 μg), the *rev* expression vector pRSV-Rev (0.5 μg), and the *gag-pol* expression vector pMDLg/pRRE (1.2 μg) using Lipofectamine 2000 (Invitrogen). At 48 h post-transfection, the culture supernatants were harvested and filtered through 0.45-μm pore size filters.

2.3. CHIP assay

The CHIP assay was performed using the ChIP-IT Express kit according to the manufacturer's recommendations (Active Motif, Carlsbad, California, USA). Briefly, 293T LTR-Luc cells (5×10^6) were plated in 100-mm dishes, washed with phosphate-buffered saline, and treated with 1% formaldehyde for 10 min. After the reaction was quenched with 0.1 M glycine, the cross-linked material was sonicated for ten pulses of 20 s each, with a 30-s rest on ice between each pulse. Immunoprecipitations were performed with protein G magnetic beads and 5 μg of either the control antibody or the anti-ZBRK1 antibody. The chromatin solution was precleared by adding protein G magnetic beads for 2 h at 4 °C. The protein G magnetic beads were blocked with 1 μg/μl of salmon sperm DNA and 1 μg/μl of bovine serum albumin overnight at 4 °C and then incubated with the chromatin and antibody for 2 h. The immunoprecipitated material was washed 3 times with the wash buffer. The cross-linking was reversed by incubating the samples for 5 h at 65 °C in 200 mM NaCl with 10 μg of RNase A to eliminate any RNA. The recovered material was treated with proteinase K and extracted using the Wizard SV Gel PCR Clean-Up System (Promega). The DNA was analyzed by quantitative PCR with *StepOne* (Applied Biosystems) and the following primers: 5′-TGA CCT TTG GAT GGT GCT TC-3′ and 5′-TCC ACA CTA ATA CTT CTC CC-3′.

2.4. Immunoprecipitation

293T cells were transfected with 0.5 μg of pNFLAG-ZBRK1 or pNFLAG-ZBRK1-DV12,13AA using Lipofectamine 2000. At 48 h post-transfection, the transfected cells were harvested and suspended in 0.5 ml of lysis buffer (20 mM Tris–HCl, pH 7.5; 250 mM NaCl; 1 mM EDTA; 5% glycerol; 1% Triton X-100). The cell lysates were centrifuged at 15,000×*g* for 20 min at 4 °C. The supernatants were incubated with 1 μg of anti-TRIM28 antibody and 40 μl of protein G-magnetic beads for 2 h at 4 °C. The beads were washed with PBS containing 0.02% Triton X-100. The immunocomplex was eluted by boiling with 20 μl of 5× sample buffer and was analyzed by SDS–PAGE and Western blotting.

2.5. MAGI assay

MAGI cells were plated in 96-well plates at 1×10^4 cells per well in Dulbecco's modified Eagle's medium with 10% fetal bovine serum. The next day, the cells were infected with dilutions of the virus in a total volume of 50 μl in the presence of 20 μg/ml of DEAE-dextran for 2 h. At 2 days post-infection, the cells were fixed with 100 μl of fixative (1% formaldehyde/0.2% glutaraldehyde in PBS) at room temperature for 5 min and then washed twice with PBS. The cells were incubated with 100 μl of staining solution (4 mM potassium ferrocyanide, 4 mM potassium ferricyanide, 2 mM $MgCl_2$, and 0.4 mg/ml X-Gal) for 50 min at 37 °C. The reaction was halted by removing the staining solution, and the blue cells were then counted using a microscope.

2.6. Real-time RT-PCR

Total RNA was extracted from shControl- or shZBRK1-transduced cells using RNeasy Mini kits (Qiagen), and cDNA was prepared with Revatra Ace (Toyobo) using oligo(dT) primers. Quantitative real-time PCR was performed with the Power SYBR Green PCR Master Mix (Applied Biosystems), and fluorescent signals were analyzed with the StepOne RT-PCR system (Applied Biosystems). The PCR primer pairs used were as follows: ZBRK1-F, 5′-AGA AAC AAG AGG CAG CCA AG-3′; ZBRK1-R, 5′-GGC TGT CCC ACA AGG ACT AC-3′; beta-actin-F, 5′-GTA CCA CTG GCA TCG TGA TGG ACT-3′; and beta-actin-R, 5′-CCG CTC ATT GCC AAT GGT GAT-3′.

2.7. Luciferase assay

The details of the luciferase assay are provided in the Supplementary Materials and methods section.

2.8. Measurement of HIV-1 p24 antigen

The details of the measurement of the p24 antigen are provided in the Supplementary Materials and methods section.

2.9. Electrophoresis mobility shift assay (EMSA)

The details of the EMSA are provided in the Supplementary Materials and methods section.

3. Results and discussion

3.1. ZBRK1 suppresses HIV-1 LTR promoter activity

We initially determined whether ZBRK1 could inhibit HIV-1 LTR promoter activity. To do this, we co-transfected 293T cells with the ZBRK1 expression vector and the HIV-1 LTR-driven luciferase reporter plasmid. Ectopic expression of ZBRK1 reduced the luciferase activity (Fig. 1A). Additionally, ZBRK1 reduced the LTR-driven luciferase mRNA level (Fig. 1B). To investigate whether ZBRK1 could repress full-length HIV-1 transcription, the viral titer of an HIV-1 molecular clone (NL4-3) produced from 293T cells expressing ZBRK1 was determined in MAGI cells. We observed that expression of ZBRK1 significantly reduced the viral titer (Fig. 1C). Moreover, we determined whether ZBRK1 could affect p24 antigen expression, which would result in a loss of viral titer. The expression of ZBRK1 resulted in a decrease in HIV-1 p24 antigen production in intracellular and culture supernatants (Fig. 1D). These results suggest that ZBRK1 represses not only the HIV-1 LTR-driven luciferase reporter plasmid but also full-length HIV-1 transcription. Next, to evaluate the function of ZBRK1 in chromatin-mediated repression of the HIV-1 LTR, we ectopically expressed ZBRK1 in HeLa cells containing an integrated LTR-luciferase reporter gene (HeLa–LTR–Luc). We then expressed HIV-1 Tat in HeLa–LTR–Luc cells, as these cells have a low basal level of luciferase activity. Expression of ZBRK1 in HeLa–LTR–Luc cells reduced the level of luciferase activity (Fig. 1E, left). To ensure that the effect observed was not due to ZBRK1-mediated suppression of Tat gene transcription, we analyzed Tat expression by Western blotting and found that ZBRK1 had no effect on the Tat expression level (Fig. 1E, right). This result demonstrates that ZBRK1 plays a significant role in chromatin-mediated repression of the HIV-1 LTR. To investigate the function of endogenous ZBRK1 in transcriptional repression of the LTR, we utilized a lentiviral vector encoding an shRNA corresponding to the ZBRK1 sequence. The expression level of endogenous ZBRK1 was reduced upon introduction of the shZBRK1-expressing lentiviral vector in 293T cells, as measured by qRT-PCR (Fig. 1F). The knockdown of ZBRK1 expression enhanced the transcriptional activity of the LTR (Fig. 1G). To further confirm the effect of endogenous ZBRK1 in HIV-1-integrated cells, 293T cells were infected with an $HIV_{NL43\text{-}luc}$ pseudotyped virus and then transduced with the shControl or shZBRK1 vectors. ZBRK1 knockdown significantly

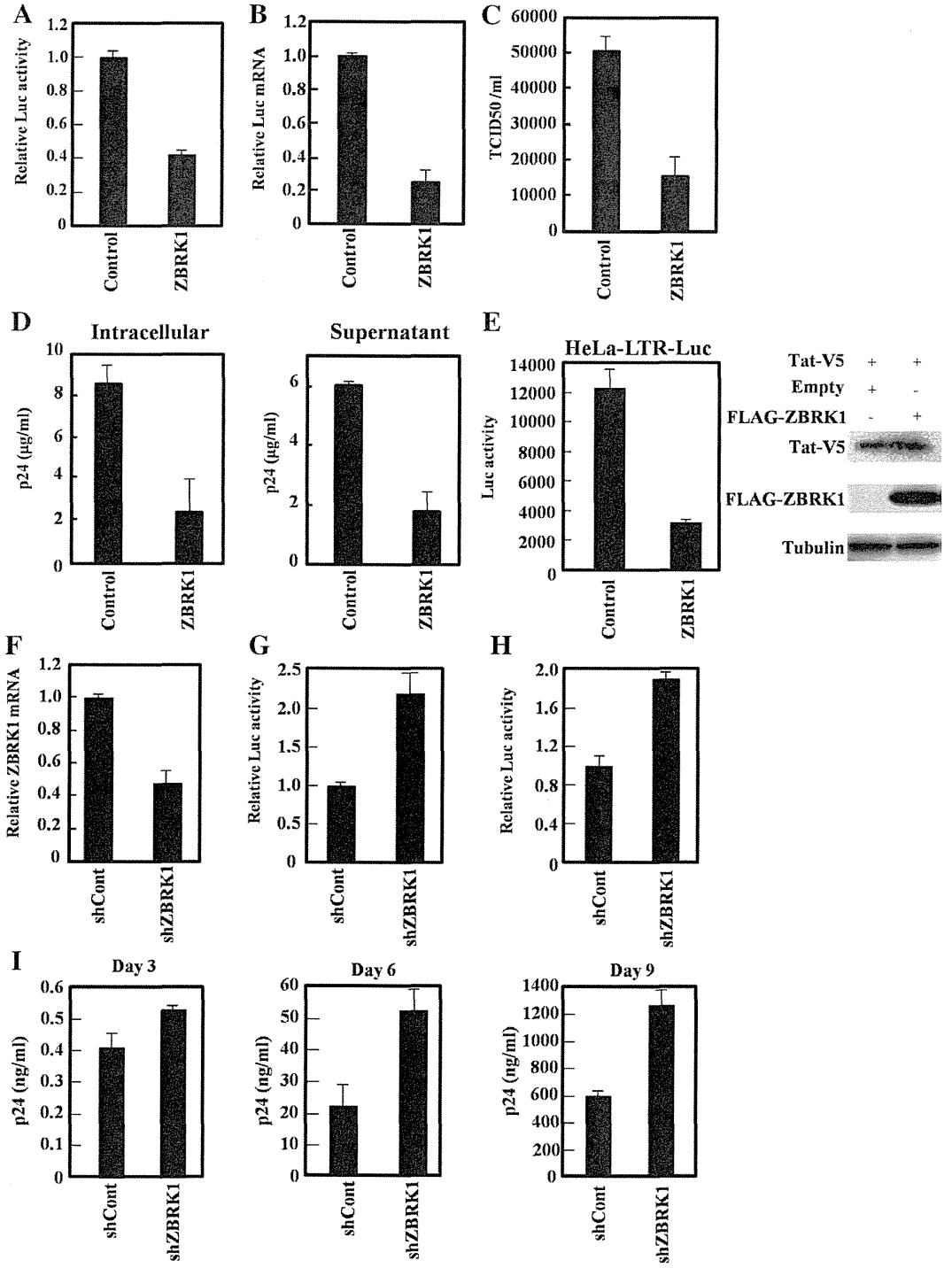

Fig. 1. ZBRK1 inhibits HIV-1 LTR-driven transcription. (A) 293T cells were transfected with 1 ng of pLTR-Luc, 1 ng of pCMV-Renilla-Luc and 200 ng of pNFLAG or pNFLAG-ZBRK1. At 48 h post-transfection, the levels of luciferase gene expression were determined by measuring the luciferase activity. Firefly luciferase activity was normalized to Renilla luciferase activity. (B) 293T cells were transfected with 200 ng of pNFLAG or pNFLAG-ZBRK1 along with 5 ng of pLTR-Luc. At 48 h post-transfection, the levels of luciferase mRNA were determined by qRT-PCR. Quantification of the beta-actin gene was performed as an internal control to correct for sample-to-sample variations in mRNA levels. (C, D) 293T cells were transfected with 200 ng of pNL4–3 and 300 ng of pNFLAG or pNFLAG-ZBRK1. At 48 h post-transfection, the virus titer (as shown, TCID50/ml (C)) were measured by MAGI assay. The amounts of p24 antigen in the intracellular compartments (D, left panel) and culture supernatants (D, right panel) were measured by a chemiluminescent enzyme immunoassay (CLEIA). (E) HeLa-LTR-Luc cells were transfected with 500 ng of pCMV-Tat-V5 and 500 ng of pNFLAG or pNFLAG-ZBRK1. At 48 h post-transfection, the cell lysates were analyzed for luciferase activity (left panel), and Tat-V5, FLAG-ZBRK1 and tubulin expression by Western blotting (right panel). (F, G) 293T cells were infected with the indicated lentiviral vectors. At 48 h post-infection, the cells were transfected with 5 ng of pLTR-Luc. At 48 h post-transfection, the levels of ZBRK1 mRNA (F) and luciferase activity (G) were determined by quantitative RT-PCR and a luciferase assay, respectively. Quantification of the beta-actin gene was performed as an internal control to correct for sample-to-sample variations in mRNA levels. (H) The pseudotyped virus was generated by co-transfection of 293T cells with 1 μg of the pNLlucΔenv and 1 μg of pMD.G. The culture supernatants were harvested at 48 h post-transfection and filtered through 0.45-μm pore size filters. 293T cells were infected with VSV-G pseudotyped NL-Luc [12]. At 1 h post-infection, 293T cells were infected with the lentiviral vectors expressing shControl or shZBRK1. At 48 h post-shRNA transduction, the levels of luciferase gene expression were determined by measuring luciferase activity. (I) MT-4 cells were infected with the lentiviral vectors expressing shControl or shZBRK1. At 5 days post-infection, the cells were infected with 2 ng of NL4-3 p24. Virus replication was monitored every 3 days after infection by measuring p24 viral antigen in the culture supernatant. The results are representative of three independent experiments, and error bars show the standard deviation of the mean values.

induced HIV-1 gene expression in the HIV-1-integrated cells (Fig. 1H). To evaluate the effect of ZBRK1 in T cells, MT-4 cells were transduced with the control or ZBRK1-specific shRNA vectors and then infected with HIV-1. Virus replication was monitored by measuring the production of p24 in the supernatant every 3 days post-infection. The depletion of ZBRK1 in MT-4 cells conferred a 2-fold enhancement on HIV-1 replication at 6 and 9 days post-infection (Fig. 1I). These results suggest that ZBRK1 inhibits HIV-1 gene expression through transcriptional repression of the LTR.

3.2. Identification of potential ZBRK1 response elements in the HIV-1 LTR

To determine the LTR sequence responsible for the suppressive function of ZBRK1, we generated deletion mutants of the LTR (Fig. 2A). The expression of ZBRK1 repressed transcription from the −335 to +282 LTR segment (Fig. 2C), the −245 to +282 LTR segment (Fig. 2D), and the full-length LTR (Fig. 2B). By contrast, repression of the LTR by ZBRK1 was abolished by the deletion of LTR sequences corresponding to −454 to −107 (Fig. 2E). These results suggest that the −454 to −107 region within the LTR contains essential elements for transcriptional repression by ZBRK1. To further define the ZBRK1-responsive region of the LTR, we constructed several more precise deletion mutants of the LTR (Fig. S1A). Similar to the wild type LTR, transcription from the LTR deletion corresponding to −205 to −146 was decreased by expression of ZBRK1 (Fig. S1B). However, deletion of the LTR corresponding to −145 to −126 partially impaired the suppressive effect of ZBRK1. These results indicate that the −145 to −126 rejoin of the LTR is a candidate for transcriptional repression by the ZBRK1.

A previous study has shown that transcriptional silencing of the HIV-1 LTR by HP1-gamma requires Sp-1, P-TEFb (which leads to the phosphorylation of RNA polymerase IICTD by recruiting HIV-1 Tat to the TAR) and PCAF (which is known to possess histone acetyl transferase activity) [13].

To further determine the role of *cis*-elements of the LTR in ZBRK1 repression, we introduced mutations into the NF-κB or Sp-1 binding sites of the LTR. However, mutations of the NF-κB and Sp-1 binding sites within the LTR did not affect ZBRK1 repression (Fig. 2F and G). In addition, HIV-1 Tat was also not required for the repressive activity of ZBRK1 (Fig. 2H). These results suggest that ZBRK1 directly represses transcriptional activity of the HIV-1 LTR.

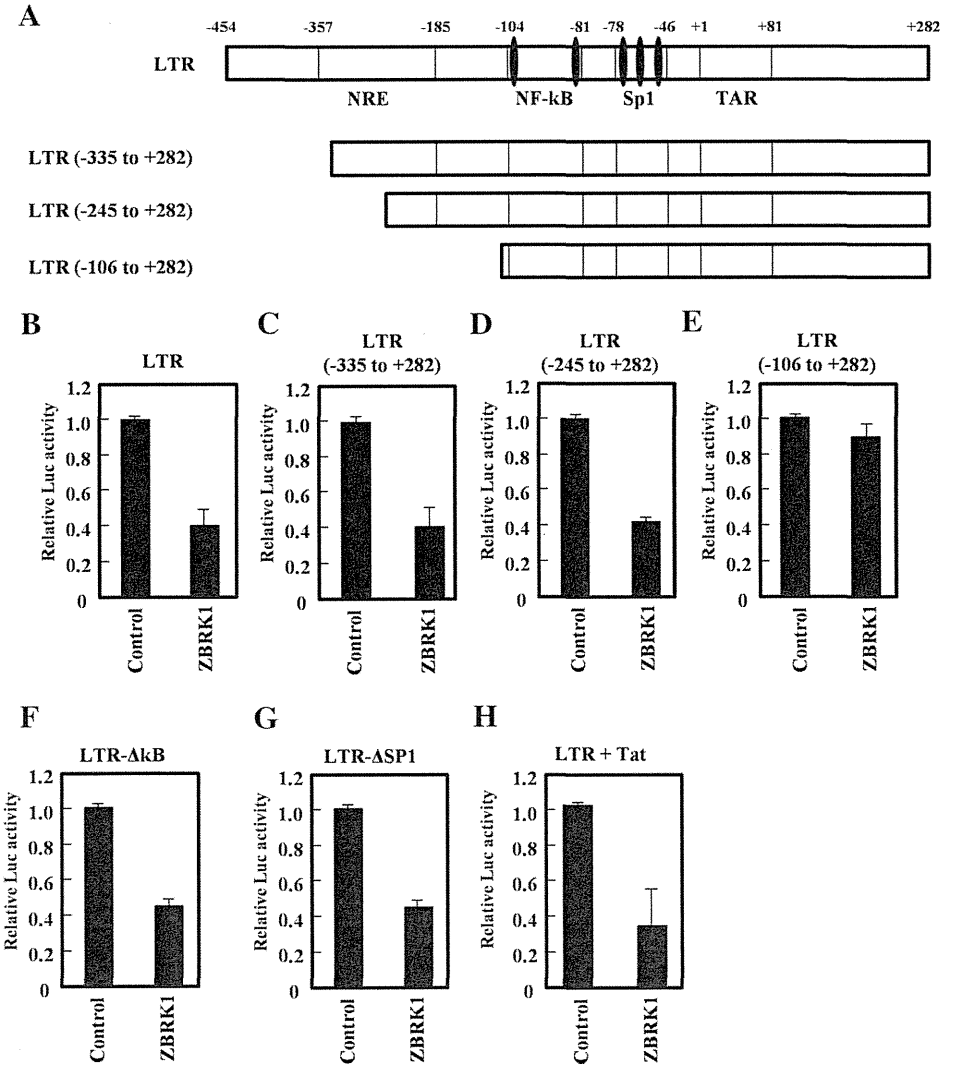

Fig. 2. The region of ZBRK1 responsible for transcriptional repression of the HIV-1 LTR. (A) A schematic representation of HIV-1 LTR-driven expression of firefly luciferase. The numbers are relative to the transcription start site nucleotide +1. (B–G) 293T cells were transfected with 1 ng of pCMV-Renilla-Luc and 200 ng of pNFLAG or pNFLAG-ZBRK1 along with 5 ng of pLTR-Luc (B) or its corresponding mutants (C–G). The luciferase assay was performed as described in Fig. 1A. (H) 293T cells were transfected with 1 ng of pCMV-Renilla-Luc, 5 ng of pLTR-Luc and 100 ng of pCMV-Tat along with 200 ng of pNFLAG or pNFLAG-ZBRK1. The luciferase assay was performed as described in Fig. 1A. The results are representative of three independent experiments, and error bars show the standard deviation of the mean values.

3.3. Transcriptional repression of the HIV-1 LTR by ZBRK1 requires TRIM28

KRAB-zinc finger proteins interact with TRIM28 through their KRAB box [14]. This interaction represses the target gene by recruiting the histone methyltransferases SETDB1 and HP1 [15]. To investigate the mechanism involved in ZBRK1-mediated repression of the LTR, we used siRNAs specific for TRIM28, HP1-gamma or SETDB1 in either empty plasmid-transfected or ZBRK1 expression plasmid-transfected cells. The introduction of each specific siRNA induced the efficient knockdown of that particular protein (Fig. 3A). The expression of ZBRK1 in siControl-transduced cells conferred a 2.4-fold repression of LTR-driven transcription (Fig. 3B). The depletion of HP1-gamma or SETDB1 had no significant effect on the ZBRK1-mediated repression of LTR transcription (Fig. 3C and D, 2.5-fold and 2.7-fold, respectively). By contrast, no repressive activity of ZBRK1 was observed in the siTRIM28-transduced cells (Fig. 3E). To further verify the TRIM28 requirement for the repressive activity of ZBRK1, we introduced two substitution mutations (DV to AA) within the KRAB domain that have previously been shown to disrupt the repressive function of KRAB domain-containing proteins. Relative to wild-type ZBRK1, ZBRK1-DV12,13AA was significantly defective in repression of LTR activity (Fig. 3F). Furthermore, FLAG-ZBRK1 was found to interact with endogenous TRIM28, but this interaction was less efficient with FLAG-ZBRK1-DV12,13AA (Fig. 3G). These results indicate that TRIM28 plays an essential role in the repressive function of ZBRK1.

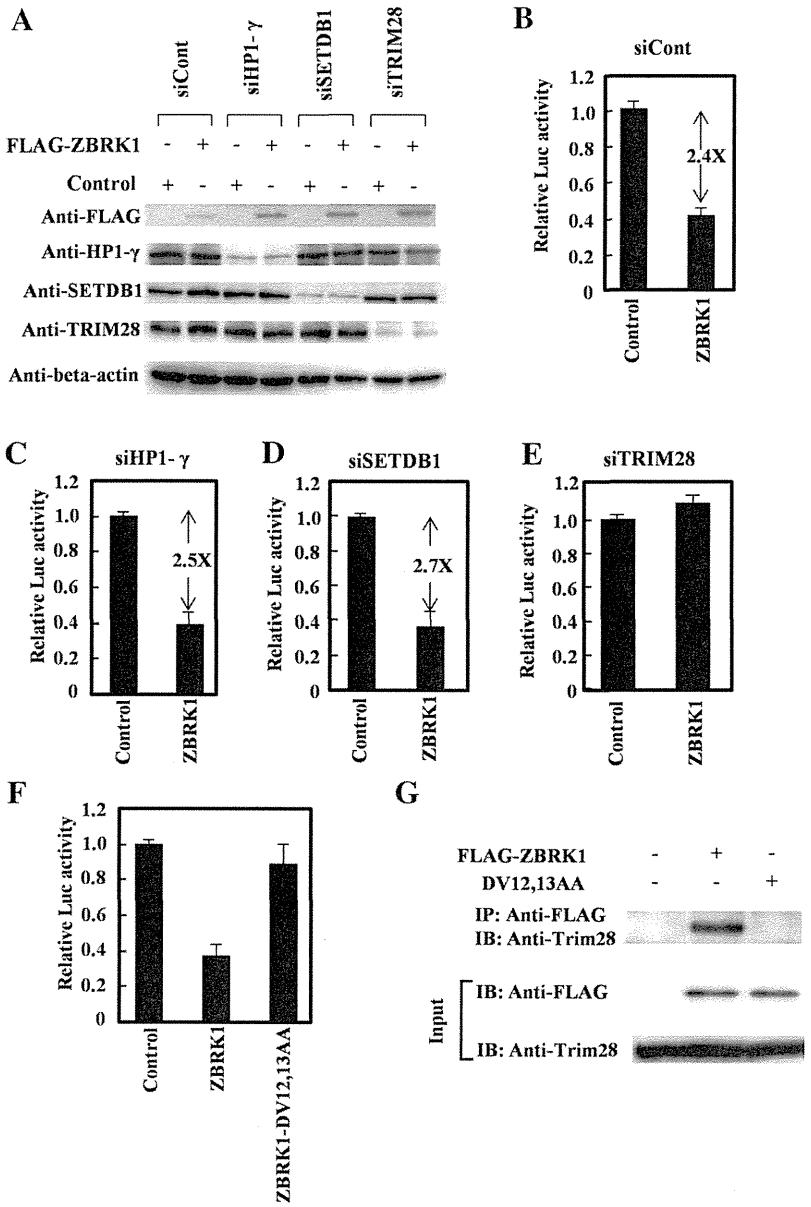

Fig. 3. TRIM28 is required for the repressive activity of ZBRK1. (A) HeLa cells were treated with 70 nM of the indicated siRNA for 24 h, prior to transfection with 5 ng of pLTR-Luc, 1 ng of pCMV-Renilla-Luc and 300 ng of pNFLAG or pNFLAG-ZBRK1. At 48 h post-transfection, the protein lysates were run on SDS–PAGE gels and probed for the indicated protein. (B–E) The protein lysates in Fig. 3A were analyzed for luciferase activity. Firefly luciferase activity was normalized to Renilla luciferase activity. The values within the graph represent the fold change of luciferase activity. (F) 293T cells were transfected with 1 ng of pCMV-Renilla-Luc and 5 ng of pLTR-Luc along with 200 ng of pNFLAG, pNFLAG-ZBRK1 or pNFLAG-ZBRK1-DV12,13AA. The luciferase assay was performed as described in Fig. 1A. (G) 293T cells were transfected with 500 ng of pNFLAG-ZBRK1 or pNFLAG-ZBRK1-DV12,13AA. At 48 h post-transfection, the cell lysates were immunoprecipitated using an anti-FLAG antibody, followed by Western blotting analysis with an anti-TRIM28 antibody. The results are representative of three independent experiments, and error bars show the standard deviation of the mean values.

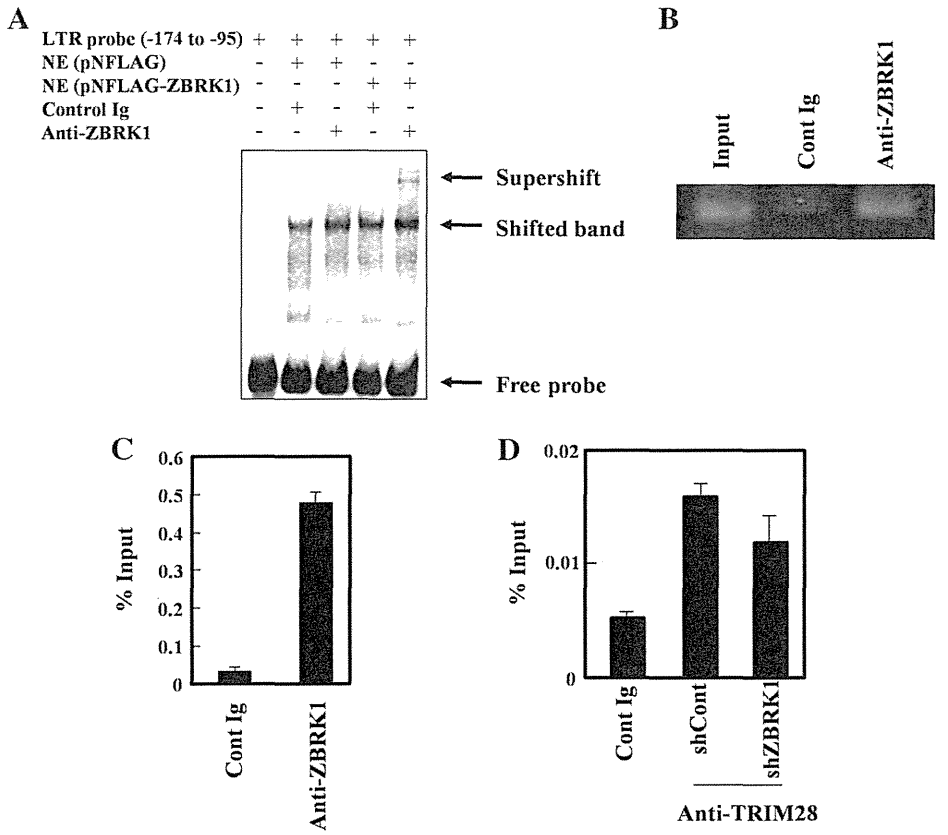

Fig. 4. ZBRK1 binds to the HIV-1 LTR in vivo. (A) An EMSA was performed by using a biotin-labeled probe corresponding to the LTR sequence (−174 to −95) and nuclear extracts from 293T cells transfected with empty plasmid or pNFLAG-ZBRK1 in the presence of control antibody or anti-ZBRK1 antibody. (B) Chromatin immunoprecipitations using anti-ZBRK1 and control Ig. PCR was performed using primers specific to the U3 region of the HIV-1 LTR. The PCR products were separated on 1.5% agarose gels and stained with SYBER Green. (C) Immunoprecipitated DNA was subjected to real-time PCR using primers specific to the U3 region of the HIV-1 LTR, as described in the materials and methods. The amount of immunoprecipitated DNA was normalized to the input DNA. The data are representative of three independent experiments. (D) The level of TRIM28 at the LTR in ZBRK1 knockdown cells.

3.4. ZBRK1 repression is histone deacetylase-dependent

As previously described, TRIM28 interacts with Mi-2alpha and other components of the NuRD complex. Additionally, TRIM28-mediated silencing requires association with NuRD and HDAC activity. By contrast, trimethylation of histone H3 on lysine 9 by SETDB1 creates high-affinity genomic binding sites for the TRIM28–HP1 complex, suggesting that SETDB1 may play an important role in TRIM28-mediated repression. However, our data indicated that SETDB1 and HP1-gamma did not affect ZBRK1-induced repression of LTR transcription (Fig. 3C and D).

To test whether histone deacetylases play a role in the repression of LTR activity by ZBRK1 in HeLa–LTR–Luc cells, we used the pan-HDAC inhibitor trichostatin A (TSA). Treatment with 400 nM of TSA significantly reversed ZBRK1-mediated repression in HeLa–LTR–Luc cells (Fig. S2A). Moreover, the repressive activity of ZBRK1 decreased in HDAC2-depleted cells (Fig. S2B). These results indicate that ZBRK1-mediated suppression of LTR activity requires HDAC2 activity.

3.5. ZBRK1 is enriched at the HIV-1 LTR

To investigate whether ZBRK1 could bind to the LTR, we performed a gel mobility shift assay using nuclear extracts from 293T cells ectopically expressing FLAG-ZBRK1. A shift of the LTR probe corresponding to LTR sequence (−175 to −95) was observed after incubation with nuclear extracts prepared from 293T cells transfected with empty plasmid or pNFLAG-ZBRK1 (Fig. 4A). However, a supershift of the labeled probe could not detect in the presence of anti-ZBRK1 antibody. This can be attributed to low levels of ZBRK1 expression in 293T cells (data not shown). In contrast, coincubation of the nuclear extracts from 293T cells expressing FLAG-ZBRK1 with anti-ZBRK1 antibody but not control antibody caused a supershift of the labeled probe. These results indicated that ZBRK1 can form a complex with HIV-1 LTR. If ZBRK1 is indeed critical for transcriptional repression of the HIV-1 LTR, it should be bound to the HIV-1 LTR in vivo. To test whether the HIV-1 LTR is bound by endogenous ZBRK1, LTR-integrated cells were analyzed by chromatin immunoprecipitation assay (CHIP assay) using an anti-ZBRK1 antibody. ZBRK1 enrichment was detected in the LTR (Fig. 4B). The level of CHIP enrichment was determined by CHIP-qPCR (Fig. 4C). In parallel, the level of binding to the housekeeping GAPDH gene was not detected by ZBRK1 enrichment (data not shown). To investigate whether ZBRK1 is required for recruitment of TRIM28 to the LTR, ZBRK1-depleted cells were analyzed by the CHIP assay using an anti-TRIM28 antibody. TRIM28 can bind to the LTR (Fig. 4D). Moreover, the depletion of ZBRK1 results in a 25% reduction in the level of TRIM28 at the LTR. These results indicate that ZBRK1 can bind to the HIV-1 LTR and partially influence recruitment of TRIM28 to the LTR. In conclusion, our data demonstrate that ZBRK1, in conjunction with TRIM28 and HDAC2, suppresses HIV-1 LTR-driven gene expression. The results of this study suggest that stimulation of KRAB-zinc finger proteins may aid in the development of antiviral therapies.

Acknowledgments

We thank Dr. H. Miyoshi for providing the lentiviral vector system, Dr. T. Suda for providing pNFLAG-Bos, Dr. I.S.Y. Chen for

providing pNL4-3lucΔenv and Yoshinori Taniguchi and Takahiro Watanabe for their technical assistance. This work was supported in part by a Grant-in-Aid for Science Research (C) from the Japan Society for the Promotion of Science (JSPS), Japan; by a Grant-in-Aid for AIDS research from the Ministry of Health, Labor, and Welfare, Japan; and by a Grant from the Strategic Research Foundation Grant-aided Project for Private Universities from the Ministry of Education, Culture, Sport, Science, and Technology, Japan (MEXT).

Appendix A. Supplementary data

Supplementary data associated with this article can be found, in the online version, at http://dx.doi.org/10.1016/j.febslet.2012.08.010.

References

[1] Rowe, H.M. et al. (2010) KAP1 controls endogenous retroviruses in embryonic stem cells. Nature 463, 237–240.
[2] Matsui, T. et al. (2010) Proviral silencing in embryonic stem cells requires the histone methyltransferase ESET. Nature 464, 927–931.
[3] Wolf, D. and Goff, S.P. (2007) TRIM28 mediates primer binding site-targeted silencing of murine leukemia virus in embryonic cells. Cell 131, 46–57.
[4] Wolf, D. and Goff, S.P. (2009) Embryonic stem cells use ZFP809 to silence retroviral DNAs. Nature 458, 1201–1204.
[5] Allouch, A., Di Primio, C., Alpi, E., Lusic, M., Arosio, D., Giacca, M. and Cereseto, A. (2011) The TRIM Family Protein KAP1 Inhibits HIV-1 Integration. Cell. Host. Microbe. 9, 484–495.
[6] Reynolds, L., Ullman, C., Moore, M., Isalan, M., West, M.J., Clapham, P., Klug, A. and Choo, Y. (2003) Repression of the HIV-1 5' LTR promoter and inhibition of HIV-1 replication by using engineered zinc-finger transcription factors. Proc. Natl. Acad. Sci. USA 100, 1615–1620.
[7] Segal, D.J., Goncalves, J., Eberhardy, S., Swan, C.H., Torbett, B.E., Li, X. and Barbas 3rd., C.F. (2004) Attenuation of HIV-1 replication in primary human cells with a designed zinc finger transcription factor. J. Biol. Chem. 279, 14509–14519.
[8] Carlson, K.A., Leisman, G., Limoges, J., Pohlman, G.D., Horiba, M., Buescher, J., Gendelman, H.E. and Ikezu, T. (2004) Molecular characterization of a putative antiretroviral transcriptional factor, OTK18. J. Immunol. 172, 381–391.
[9] Zheng, L., Pan, H., Li, S., Flesken-Nikitin, A., Chen, P.L., Boyer, T.G. and Lee, W.H. (2000) Sequence-specific transcriptional corepressor function for BRCA1 through a novel zinc finger protein, ZBRK1. Mol. Cell. 6, 757–768.
[10] Zhou, H. et al. (2008) Genome-scale RNAi screen for host factors required for HIV replication. Cell. Host. Microbe. 4, 495–504.
[11] Furuta, S. et al. (2006) Removal of BRCA1/CtIP/ZBRK1 repressor complex on ANG1 promoter leads to accelerated mammary tumor growth contributed by prominent vasculature. Cancer. Cell. 10, 13–24.
[12] Planelles, V., Bachelerie, F., Jowett, J.B., Haislip, A., Xie, Y., Banooni, P., Masuda, T. and Chen, I.S. (1995) Fate of the human immunodeficiency virus type 1 provirus in infected cells: a role for vpr. J. Virol. 69, 5883–5889.
[13] du Chene, I. et al. (2007) Suv39H1 and HP1gamma are responsible for chromatin-mediated HIV-1 transcriptional silencing and post-integration latency. EMBO. J. 26, 424–435.
[14] Friedman, J.R., Fredericks, W.J., Jensen, D.E., Speicher, D.W., Huang, X.P., Neilson, E.G. and Rauscher 3rd., F.J. (1996) KAP-1, a novel corepressor for the highly conserved KRAB repression domain. Genes. Dev. 10, 2067–2078.
[15] Nielsen, A.L., Ortiz, J.A., You, J., Oulad-Abdelghani, M., Khechumian, R., Gansmuller, A., Chambon, P. and Losson, R. (1999) Interaction with members of the heterochromatin protein 1 (HP1) family and histone deacetylation are differentially involved in transcriptional silencing by members of the TIF1 family. EMBO. J. 18, 6385–6395.

Bioorganic & Medicinal Chemistry Letters 23 (2013) 503–506

Contents lists available at SciVerse ScienceDirect

Bioorganic & Medicinal Chemistry Letters

journal homepage: www.elsevier.com/locate/bmcl

2′-Fluoro-6′-methylene-carbocyclic adenosine phosphoramidate (FMCAP) prodrug: In vitro anti-HBV activity against the lamivudine–entecavir resistant triple mutant and its mechanism of action

Ravindra K. Rawal [a], Uma S. Singh [a], Satish N Chavre [a], Jianing Wang [a], Masaya Sugiyama [b], Wai Hung [a], Rajgopal Govindarajan [a], Brent Korba [c], Yasuhito Tanaka [b], Chung K. Chu [a,*]

[a] The University of Georgia, College of Pharmacy, Athens, GA 30602, USA
[b] Nagoya City University Graduate School of Medical Sciences, Nagoya 467 8601, Japan
[c] Georgetown University Medical Center, WA 20057, USA

ARTICLE INFO

Article history:
Received 28 September 2012
Accepted 8 November 2012
Available online 24 November 2012

Keywords:
Carbocyclic-nucleos(t)ide
Anti-HBV activity
Wild-type
Lamivudine–entecavir triple mutant
Drug-resistant mutants

ABSTRACT

Novel 2′-fluoro-6′-methylene-carbocyclic adenosine (FMCA) monophosphate prodrug (FMCAP) was synthesized and evaluated for its in vitro anti-HBV potency against a lamivudine–entecavir resistant clone (L180M + M204V + S202G). FMCA demonstrated significant antiviral activity against wild-type as well as lamivudine–entecavir resistant triple mutant (L180M + M204V + S202G). The monophosphate prodrug (FMCAP) demonstrated greater than 12-fold (12×) increase in anti-HBV activity without increased cellular toxicity. Mitochondrial and cellular toxicity studies of FMCA indicated that there is no significant toxicity up to 100 μM. Mode of action studies by molecular modeling indicate that the 2′-fluoro moiety by hydrogen bond as well as the Van der Waals interaction of the carbocyclic ring with the phenylalanine moiety of the polymerase promote the positive binding, even in the drug-resistant mutants.

The chronic HBV infection is strongly associated with liver diseases like chronic hepatic insufficiency, cirrhosis and hepatocellular carcinoma (HCC).[1] According to the World Health Organization (WHO), currently about 2 billion people world-wide have been infected with HBV and more than 350 million live with chronic infection. Acute or chronic outcomes of HBV infection are estimated to cause the deaths of 600,000 people worldwide every year.[2]

Currently, there are several nucleos(t)ide analogues available to treat chronic hepatitis B virus infection.[3–6] The major target of these drugs is to inhibit the viral reverse transcriptase (RT)/DNA polymerase, which is responsible for the synthesis of the minus-strand DNA. Although the currently used agents are well tolerated and effective in suppressing the viral replication for extended periods, the significant rate of virological relapse caused by drug resistance remains a critical issue.

Lamivudine (LVD) was first introduced as the orally active anti-HBV agent in 1998. Lamivudine profoundly suppresses HBV replication in patients with chronic hepatitis B infection; however, lamivudine-resistant HBV (LVDr) was isolated from a significant numbers of patients during the treatment with lamivudine. Currently, there are several antiviral options exist for these patients viz., to use adefovir or high dose (1.0 mg/day) of entecavir, or more recently tenofovir. However, this resulted in also the development of resistance mutants during the long term therapy. At present, entecavir is the most prescribed drug, and is recommended for patients with the wild-type as well as for those harboring adefovir and lamivudine-resistant strains. However, recent clinical studies by Tanaka and his co-workers suggested that the entecavir mutant in the lamivudine-resistant patients (L180M + M204V + S202G) causes a viral breakthrough: 4.9% of patients at baseline increases to 14.6%, 24% and 44.8% at weeks 48, 96 and 144, respectively.[7] Therefore, it is of great interest to discover novel anti-HBV agent, which is effective against lamivudine- and entecavir-resistant triple mutants (L180M + M204V + S202G).

The potency of a nucleos(t)ide analogue is determined by its ability to serve as a competitive inhibitor of the HBV polymerase relative to that of the natural substrate, the nucleotide triphosphate.[8] However, host cellular kinases limit the pharmacological potency of nucleoside analogues by phosphorylation to their corresponding triphosphates. Particularly, the initial kinase action on the nucleoside to the monophosphate is the rate-limiting step. However, many synthetic nucleosides are not phosphorylated or the rate of phosphorylation is very slow due to the structural requirement of the kinases, resulting in only generating a low quantity of the triphosphate. To overcome this phosphorylation issue, nucleoside phosphoramidate prodrugs have been introduced,[8,9] which

* Corresponding author. Address: Department of Pharmaceutical and Biomedical Sciences, College of Pharmacy, The University of Georgia, Athens, GA 30602, USA. Tel.: +1 706 542 5379; fax: +1 706 542 5381.
E-mail address: DCHU@rx.uga.edu (C.K. Chu).

0960-894X/$ - see front matter © 2012 Elsevier Ltd. All rights reserved.
http://dx.doi.org/10.1016/j.bmcl.2012.11.027

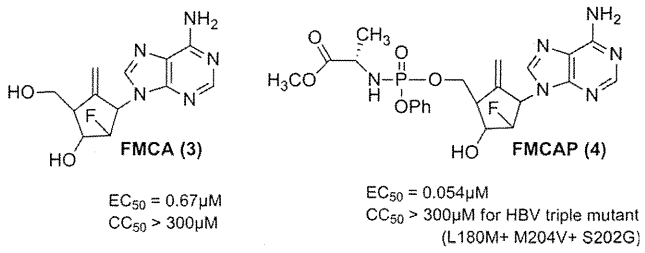

Figure 1. Structures of 2′-fluoro-6′-methylene-carbocyclic adenosine (FMCA; **3**) and its prodrug (FMCAP; **4**).

can bypass the rate-limiting first step of monophosphorylation. Phosphoramidate prodrugs have demonstrated to enhance the nucleoside potency in cell culture as well as in patients.[10,11] This methodology greatly increases the lipophilicity of the nucleotide to increase the cell penetration as well as to target the liver cells in vivo.

In this communication, we present that a FMCA phosphoramidate prodrug is such an agent, which can potentially be used for the treatment of patients who experience viral breakthrough due to the triple mutants caused by the use of lamivudine and entecavir.

In our previous report, we have demonstrated that the novel carbocyclic adenosine analog **3** (FMCA Fig. 1) exhibits significant anti-HBV activity against wild type as well as adefovir/lamivudine resistant strains.[12] The present study describes the synthesis and antiviral evaluation of a phosphoramidate of FMCA (FMCAP), which demonstrated the significantly improved in vitro potency. Additionally, we studied its mechanism of action how FMCA-TP can effectively bind to the HBV polymerase by molecular modeling and still exerts the antiviral activity against the lamivudine–entecavir triple mutant (L180M + M204V + S202G).

FMCAP (**4**, Scheme 1)[13] was synthesized using a known method in the literature,[14,15] in which the phosphorylation of phenol with phosphorus oxychloride generates phenyl dichlorophosphate **1**, which was coupled with L-alanine methyl ester in the presence of *tri*-ethyl amine in dichloromethane to give chlorophosphoramidate reagent **2**, which, in turn, was coupled with FMCA **3** in the presence of 1-methyl imidazole in THF to furnish the phosphoramidate **4** in good yield.

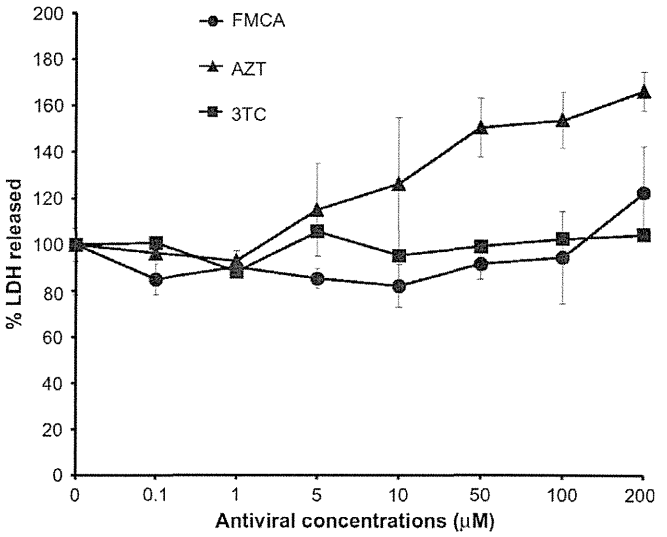

Figure 2. Mitochondrial toxicity of FMCA **3**, AZT and 3TC through lactate dehydrogenase release (LDH) assay.

FMCA **3** and FMCAP **4** were evaluated in vitro against the wild-type as well as the lamivudine–entecavir resistant clone (L180M + S202I + M202V). The FMCA **3** and FMCAP **4** demonstrated significant anti-HBV activity (EC_{50} 0.548 ± 0.056 & 0.062 ± 0.011 μM, respectively) against the wild-type virus, while lamivudine and entecavir also demonstrated potent anti-HBV activity (EC_{50} 0.056 ± 0.003 & 0.008 μM, respectively) (Table 1). It is noteworthy to mention that the anti-HBV potency of FMCAP (**4**) was increased to eight-fold (8×) in comparison to that of FMCA **3**, which indicates the importance of the initial phosphorylation of the nucleoside.

FMCA **3** and FMCAP **4** were further evaluated for their in-vitro antiviral potency against a lamivudine–entecavir resistant clone (L180M + M204V + S202G). It was observed that the anti-HBV potency of both FMCA **3** and FMCAP **4** (EC_{50} 0.67 & 0.054 μM, respectively) were maintained against the resistant clone, and furthermore, the anti-HBV activity of FMCAP **4** was enhanced a 12-fold (12×) with respect to that of FMCA without significant enhancement of cellular toxicity. It was also noteworthy to mention that the anti-HBV potency of entecavir against the mutant

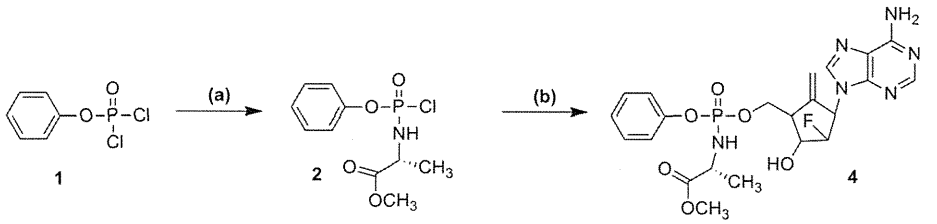

Scheme 1. Reagent and conditions: (a) L-alanine methyl ester hydrochloride, Et_3N, CH_2Cl_2; (b) FMCA (3), NMI, THF, rt overnight.

Table 1
In vitro anti-HBV activity of FMCA **3**, FMCAP **4**, lamivudine and entecavir against wild-type and entecavir drug-resistant mutant (L180M + M204V + S202G) in Huh7 cells

Compounds	HBV Strains			
	Wild-type			L180M + M204V + S202G
	EC_{50} (μM)	EC_{90} (μM)	CC_{50} (μM)	EC_{50} (μM)
FMCA **3**	0.548 ± 0.056	6.0 ± 0.400	>300	0.67
FMCAP **4**	0.062 ± 0.011	0.46 ± 0.060	>300	0.054
Lamivudine	0.056 ± 0.003	0.142 ± 0.008	>300	>500[17]
Entecavir	0.008	0.033	28	1.20[16]

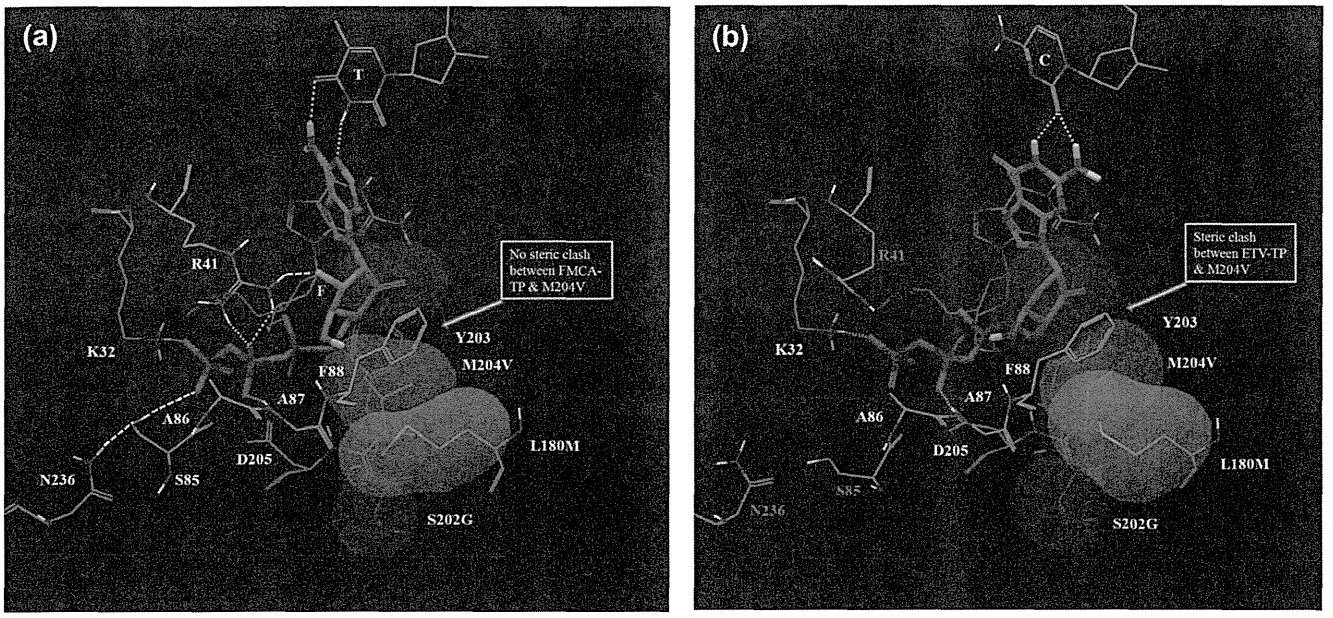

Figure 3. (a) FMCA-TP binding mode in ETVr (L180M + M204V + S202G); and (b) ETV-TP binding mode in ETVr (L180M + M204V + S202G) and there is a steric hindrance. Yellow dotted lines are hydrogen bonding interactions (<2.5 Å). The Van der Waals surface of L180M is colored yellow. The Van der Waals surface of M204V is shown in spring green. The Van der Waals surface of S202G is colored orange. The exocyclic double bond is shown blue color.

Table 2
MBAE (multi-ligand bimolecular association with energetics) calculation of FMCA-TP and ETV-TP after Glide XP docking[21] and energy minimization[22]

Strains	Compounds	Energy difference results (ΔE, kcal/mol)		
		Total energy	VdW[a]	Electrostatic
Wild-type	FMCA-TP	−588.05	375.78	−6341.08
	ETV-TP	−597.25	350.35	−6009.65
ETVr	FMCA-TP	−591.54	359.91	−6245.68
(L180M + M204V + S202G)	ETV-TP	−320.28	248.82	−4831.12

[a] Van der Waals interaction.

was reduced by 150-fold (EC_{50} 1.2 μM) in comparison to wild type.[16]

In the preliminary mitochondrial toxicity studies in HepG2 cells by measuring the lactic dehydrogenase release,[18] FMCA **3** did not exhibit any significant toxicity up to 100 μM like lamivudine (3TC), while azidothymidine (AZT) shows the increase of toxicity (Fig. 2).

In our previous report, we described molecular modeling studies for favorable anti-HBV activity of FMCA-TP in wild-type as well as in N236T adefovir resistant (ADVr) mutant.[12] In the current studies, it was of interest to know how the FMCA and its prodrug maintain the anti-HBV activity against ETVr triple mutant (L180M + M204V + S202G) in comparison to entecavir. Therefore, molecular modeling studies were conducted to obtain the insight of the molecular mechanism of FMCA-TP by using the Schrodinger Suite modules.[19] A previously described homology model was used to further explore the impact of the ETVr to the HBV-RT.[12] The homology model of HBV-RT was constructed based on the published X-ray crystal structure of HIV reverse transcriptase (PDB code: 1RTD).[20]

The binding mode of FMCA-TP and ETV-TP in ETVr (L180M + M204V + S202G) HBV-RT are depicted in Figure 3a and b, respectively. Their MBAE (multi-ligand biomolecular association with energetics)[22] calculations of FMCA-TP (total energy, wt −588.05 & ETVr −591.54 kcal/mol) and ETV-TP (total energy, wt −597.25 & ETVr −320.28 kcal/mol) after glide XP (extra precision) docking[21] and energy minimization in ETVr HBV-RT are shown in Table 2. The triphosphate of FMCA-TP forms all the network of hydrogen bonds with the active site residues (Fig. 3a), K32, R41, S85 & A87 in the similar manner as in wild-type,[12] whereas ETV-TP lose the hydrogen bonding with R41 & S85. The γ-phosphate of FMCA-TP maintains a critical H-bonding with the OH of S85 with connection of hydrogen bonds between S85 and N236 in ETVr HBV-RT also. However, γ-phosphate ETV-TP does not maintain this critical H-bonding with S85 and N236 (Fig. 3b).

The carbocyclic ring with an exocyclic double bond of FMCA-TP and ETV-TP makes the favorable Van der Waals interaction with F88 in ETVr HBV-RT (Fig. 3a and b). There is no steric clash in between exocyclic double bond of FMCA-TP and M204V residue, whereas ETV-TP exocyclic double bond has steric clash with M204V residue in ETVr HBV-RT. The 2′-fluorine substituent in the carbocyclic ring of FMCA-TP appears to promote an additional binding with the NH of R41 guanidino group as shown in Figure 3a, which is in agreement with the antiviral activity of FMCA-TP shown in Table 1. Overall, the modeling studies can qualitatively explain the favorable anti-HBV activity of FMCA-TP against ETVr mutant (L180M + M204V + S202G) in comparison to entecavir as shown in Table 1.

In conclusion, 2′-fluoro-6′-methylene-carbocyclic adenosine phosphoramidate prodrug (FMCAP) was synthesized, which demonstrated the significantly increased anti-HBV potency relative to the parent compound, FMCA in vitro. Molecular modeling studies delineated the mechanism of FMCA-TP and how it can effectively bind to the lamivudine–entecavir resistant triple mutant resulting

in maintaining the anti-HBV activity against the mutant. Furthermore, FMCA has been studied for the release of lactic dehydrogenase for potential mitochondrial toxicity and found that no significant increase of toxicity of FMCA compared with other commonly used anti-HIV nucleoside drugs. Very recently, a preliminary in vivo study in chimeric mice harboring the triple mutant, FMCAP was found to reduce HBV viral load while entecavir did not (data not shown). In view of these promising anti-HBV activities and non-toxicity of FMCAP as well as the interesting mechanism of antiviral activity, the chiral synthesis of FMCAP and its mitochondrial toxicity studies for preclinical investigation are warranted.

Acknowledgment

This research was supported by the U.S. Public Health Service Grant AI-25899 (C.K.C.), NOI-AI-30046 (B.K.) from the National Institute of Allergy and Infectious Diseases, NIH.

References and notes

1. El-Serag, H. B. *N. Engl. J. Med.* **2011**, *365*, 1118.
2. http://www.who.int/mediacentre/factsheets/fs204/en/.
3. Sharon, A.; Jha, A. K.; Chu, C. K. *Analogue-Based Drug Discovery II*, 383.
4. Jarvis, B.; Faulds, D. *Drugs* **1999**, *58*, 101.
5. Marcellin, P.; Chang, T.; Lim, S. G.; Tong, M. J.; Sievert, W.; Shiffman, M. L.; Jeffers, L.; Goodman, Z.; Wulfsohn, M. S.; Xiong, S.; Fry, J.; Brosgart, C. L. *N. Engl. J. Med.* **2003**, *348*, 808.
6. Pol, S.; Lampertico, P. *J. Viral Hepat.* **2012**, *19*, 377.
7. Mukaide, M.; Tanaka, Y.; Shin, T.; Yuen, M. F.; Kurbanov, F.; Yokosuka, O.; Sata, M.; Karino, Y.; Yamada, G.; Sakaguchi, K. *Antimicrob. Agents Chemother.* **2010**, *54*, 882.
8. Hecker, S. J.; Erion, M. D. *J. Med. Chem.* **2008**, *51*, 2328.
9. Sofia, M. J.; Bao, D.; Chang, W.; Du, J.; Nagarathnam, D.; Rachakonda, S.; Reddy, P. G.; Ross, B. S.; Wang, P.; Zhang, H.-R.; Bansal, S.; Espiritu, C.; Keilman, M.; Lam, A. M.; Steuer, H. M. M.; Niu, C.; Otto, M. J.; Furman, P. A. *J. Med. Chem.* **2010**, *53*, 7202.
10. Chang, W.; Bao, D.; Chun, B.-K.; Naduthambi, D.; Nagarathnam, D.; Rachakonda, S.; Reddy, P. G.; Ross, B. S.; Zhang, H.-R.; Bansal, S.; Espiritu, C. L.; Keilman, M.; Lam, A. M.; Niu, C.; Steuer, H. M.; Furman, P. A.; Otto, M. J.; Sofia, M. J. *ACS Med. Chem. Lett.* **2010**, *2*, 130.
11. McGuigan, C.; Gilles, A.; Madela, K.; Aljarah, M.; Holl, S.; Jones, S.; Vernachio, J.; Hutchins, J.; Ames, B.; Bryant, K. D.; Gorovits, E.; Ganguly, B.; Hunley, D.; Hall, A.; Kolykhalov, A.; Liu, Y.; Muhammad, J.; Raja, N.; Walters, R.; Wang, J.; Chamberlain, S.; Henson, G. *J. Med. Chem.* **2010**, *53*, 4949.
12. Wang, J.; Singh, U. S.; Rawal, R. K.; Sugiyama, M.; Yoo, J.; Jha, A. K.; Scroggin, M.; Huang, Z.; Murray, M. G.; Govindarajan, R. *Bioorg. Med. Chem. Lett.* **2011**, *21*, 6328.
13. *Compound* **4**: ^{1}H NMR (500 Mz, $CDCl_3$) δ 8.35 (s, 1H), 7.86 (d, J = 3.0 Hz, 1H), 7.34–7.15 (m, 5H), 5.95 (m, 3H), 5.26 (d, J = 8.0 Hz, 1H), 5.01–4.90 (m, 1H), 4.83 (s, 1H), 4.50–4.41 (m, 2H), 4.25–4.04 (m, 3H), 3.71 (s, 3H), 3.07 (s, 1H), 1.40 (d, J = 6.5 Hz, 3 H); ^{19}F NMR (500 MHz, $CDCl_3$) δ −192.86 (m, 1F); ^{13}C NMR (125 MHz, $CDCl_3$) δ 171, 159.0, 156.5, 152.5, 150.4, 142.9, 130.1, 121.2, 120.3, 106.7, 102.4, 72.2, 71.1, 62.3, 51.9, 46.3, 43.9, 19.1; ^{31}P NMR (202 MHz, $CDCl_3$): δ 2.67, 2.99. Anal. Calcd For $C_{22}H_{26}FN_6O_6P.0.5H_2O$: C, 49.91; H, 5.14; N, 15.87; Found C, 49.84; H, 5.06; N, 15.22.
14. McGuigan, C.; Pathirana, R. N.; Mahmood, N.; Devine, K. G.; Hay, A. J. *Antiviral Res.* **1992**, *17*, 311.
15. Liang, Y.; Narayanasamy, J.; Schinazi, R. F.; Chu, C. K. *Bioorg. Med. Chem.* **2006**, *14*, 2178.
16. Walsh, A. W.; Langley, D. R.; Colonno, R. J.; Tenney, D. J. *PloS one* **2010**, *5*, e9195.
17. Villet, S.; Ollivet, A.; Pichoud, C.; Barraud, L.; Villeneuve, J. P.; Trépo, C.; Zoulim, F. *J. Hepatol.* **2007**, *46*, 531.
18. Lai, Y.; Tse, C. M.; Unadkat, J. D. *J. Biol. Chem.* **2004**, *279*, 4490.
19. Schrodinger Suite 2012; LLC, NY, 2012.
20. http://www.rcsb.org/pdb.
21. Glide version 5.8; Schrodinger LLC, NY, 2012.
22. Macromodel version 9.9; Schrodinger LLC, NY, 2012.

PLOS ONE

Soluble MICA and a *MICA* Variation as Possible Prognostic Biomarkers for HBV-Induced Hepatocellular Carcinoma

Vinod Kumar[1,2]*, Paulisally Hau Yi Lo[1], Hiromi Sawai[3], Naoya Kato[4], Atsushi Takahashi[2], Zhenzhong Deng[1], Yuji Urabe[1], Hamdi Mbarek[1], Katsushi Tokunaga[3], Yasuhito Tanaka[5], Masaya Sugiyama[6], Masashi Mizokami[6], Ryosuke Muroyama[4], Ryosuke Tateishi[7], Masao Omata[7], Kazuhiko Koike[7], Chizu Tanikawa[1], Naoyuki Kamatani[2], Michiaki Kubo[2], Yusuke Nakamura[1], Koichi Matsuda[1]

1 Laboratory of Molecular Medicine, Human Genome Center, Institute of Medical Science, The University of Tokyo, Tokyo, Japan, **2** Center for Genomic Medicine, The Institute of Physical and Chemical Research (RIKEN), Kanagawa, Japan, **3** Department of Human Genetics, Graduate School of Medicine, The University of Tokyo, Tokyo, Japan, **4** Unit of Disease Control Genome Medicine, The Institute of Medical Science, The University of Tokyo, Tokyo, Japan, **5** Department of Clinical Molecular Informative Medicine, Nagoya City University Graduate School of Medical Sciences, Aichi, Japan, **6** The Research Center for Hepatitis and Immunology, National Center for Global Health and Medicine, Chiba, Japan, **7** Department of Gastroenterology, Graduate School of Medicine, The University of Tokyo, Tokyo, Japan

Abstract

MHC class I polypeptide-related chain A (MICA) molecule is induced in response to viral infection and various types of stress. We recently reported that a single nucleotide polymorphism (SNP) rs2596542 located in the *MICA* promoter region was significantly associated with the risk for hepatitis C virus (HCV)-induced hepatocellular carcinoma (HCC) and also with serum levels of soluble MICA (sMICA). In this study, we focused on the possible involvement of MICA in liver carcinogenesis related to hepatitis B virus (HBV) infection and examined correlation between the *MICA* polymorphism and the serum sMICA levels in HBV-induced HCC patients. The genetic association analysis revealed a nominal association with an SNP rs2596542; a G allele was considered to increase the risk of HBV-induced HCC ($P = 0.029$ with odds ratio of 1.19). We also found a significant elevation of sMICA in HBV-induced HCC cases. Moreover, a G allele of SNP rs2596542 was significantly associated with increased sMICA levels ($P = 0.009$). Interestingly, HCC patients with the high serum level of sMICA (>5 pg/ml) exhibited poorer prognosis than those with the low serum level of sMICA (≤5 pg/ml) ($P = 0.008$). Thus, our results highlight the importance of *MICA* genetic variations and the significance of sMICA as a predictive biomarker for HBV-induced HCC.

Citation: Kumar V, Yi Lo PH, Sawai H, Kato N, Takahashi A, et al. (2012) Soluble MICA and a *MICA* Variation as Possible Prognostic Biomarkers for HBV-Induced Hepatocellular Carcinoma. PLoS ONE 7(9): e44743. doi:10.1371/journal.pone.0044743

Editor: Erica Villa, University of Modena & Reggio Emilia, Italy

Received May 3, 2012; **Accepted** August 7, 2012; **Published** September 14, 2012

Funding: This work was conducted as a part of the BioBank Japan Project that was supported by the Ministry of Education, Culture, Sports, Science and Technology of the Japanese government. The funders had no role in study design, data collection and analysis, decision to publish, or preparation of the manuscript.

Competing Interests: The authors have declared that no competing interests exist.

* E-mail: koichima@ims.u-tokyo.ac.jp

Introduction

Hepatocellular carcinoma (HCC) reveals a very high mortality rate that is ranked the third among all cancers in the world [1]. HCC is known to develop in a multistep process which has been related to various risk factors such as genetic factors, environment toxins, alcohol and drug abuse, autoimmune disorders, elevated hepatic iron levels, obesity, and hepatotropic viral infections [2]. Among them, chronic infection with hepatitis B virus (HBV) is one of the major etiological factors for developing HCC with considerable regional variations ranging from 20% of HCC cases in Japan to 65% in China [3].

Interestingly, clinical outcome after the exposure to HBV considerably varies between individuals. The great majority of individuals infected with HBV spontaneously eliminate the viruses, but a subset of patients show the persistent chronic hepatitis B infection (CHB), and then progresses to liver cirrhosis and HCC through a complex interplay between multiple genetic and environmental factors [4]. In this regard, genome wide association studies (GWAS) using single nucleotide polymorphisms (SNPs) have highlighted the importance of genetic factors in the pathogenesis of various diseases including CHB as well as HBV-induced HCC [5,6,7,8,9,10,11,12,13]. Recently, we identified a genetic variant located at 4.7 kb upstream of the *MHC class I polypeptide-related chain A* (*MICA*) gene to be strongly associated with hepatitis C virus (HCV) -induced HCC development [14].

MICA is highly expressed on viral-infected cells or cancer cells, and acts as ligand for NKG2D to activate antitumor effects of Natural killer (NK) cells and $CD8^+$ T cells [15,16]. Our previous results indicated that a G allele of SNP rs2596542 was significantly associated with the lower cancer risk and the higher level of soluble MICA (sMICA) in the serum of HCV-induced HCC patients, demonstrating the possible role of MICA as a tumor suppressor. However, elevation of serum sMICA was shown to be associated with poor prognosis in various cancer patients [17,18,19,20].

Matrix metalloproteinases (MMPs) can cleave MICA at a transmembrane domain [21] and release sMICA proteins from cells. Since sMICA was shown to inhibit the antitumor effects of NK cells and $CD8^+$ T cells by reduction of their affinity to binding to target cells [22,23], the effect of MICA in cancer cells would be modulated by the expression of MMPs. To elucidate the role of MICA in HBV-induced hepatocellular carcinogenesis, we here report analysis of the *MICA* polymorphism and serum sMICA level in HBV-induced HCC cases.

Materials and Methods

Study participants

The demographic details of study participants are summarized in Table 1. A total of 181 HCC cases, 597 CHB patients, and 4,549 non-HBV controls were obtained from BioBank Japan that was initiated in 2003 with the funding from the Ministry of Education, Culture, Sports, Science and Technology, Japan [24]. In the Biobank Japan Project, DNA and serum of patients with 47 diseases were collected through collaborating network of 66 hospitals throughout Japan. List of participating hospitals is shown in the following website (http://biobankjp.org/plan/member_hospital.html). A total of 226 HCC cases, 102 CHB patients, and 174 healthy controls were additionally obtained from the University of Tokyo. The diagnosis of chronic hepatitis B was conducted on the basis of HBsAg-seropositivity and elevated serum aminotransferase levels for more than six months according to the guideline for diagnosis and treatment of chronic hepatitis (The Japan Society of Hepatology, http://www.jsh.or.jp/medical/gudelines/index.html). Control Japanese DNA samples (n = 934) were obtained from Osaka-Midosuji Rotary Club, Osaka, Japan. All HCC patients were histopathologically diagnosed. Overall survival was defined as the time from blood sampling for sMICA test to the date of death due to HCC. Patients who were alive on the date of last follow-up were censored on that date. All participants provided written informed consent. This research project was approved by the ethics committee of the University of Tokyo and the ethics committee of RIKEN. All clinical assessments and specimen collections were conducted according to Declaration of Helsinki principles.

SNP genotyping

Genotyping platforms used in this study were shown in Table 1. We genotyped 181 HCC cases and 5,483 non-HBV control samples using either Illumina Human Hap610-Quad or Human Hap550v3. The other samples were genotyped at SNP rs2596542 by the Invader assay system (Third Wave Technologies, Madison, WI).

MICA variable number tandem repeat (VNTR) locus genotyping

Genotyping of the *MICA* VNTR locus in 176 HBV-induced HCC samples was performed using the primers reported previously by the method recommended by Applied Biosystems (Foster City, CA) [14]. Briefly, the 5′ end of forward primer was labeled with 6-FAM, and reverse primer was modified with GTGTCTT non-random sequence at the 5′ end to promote Plus A addition. The PCR products were mixed with Hi-Di Formamide and GeneScan-600 LIZ size standard, and separated by GeneScan system on a 3730×l DNA analyzer (Applied Biosystems, Foster City, CA). GeneMapper software (Applied Biosystems, Foster City, CA) was employed to assign the repeat fragment size (Figure S1).

Quantification of soluble MICA

We obtained serum samples of 111 HBV-positive HCC samples, 129 HCV-positive HCC samples, and 60 non-HBV controls from Biobank Japan. Soluble MICA levels were measured by sandwich enzyme-linked immunosorbent assay, as described in the manufacturer's instructions (R&D Systems, Minneapolis, MN).

Statistical analysis

The association between an SNP rs2596542 and HBV-induced HCC was tested by Cochran-Armitage trend test. The Odds ratios were calculated by considering a major allele as a reference. Statistical comparisons between genotypes and sMICA levels were performed by Kruskal-Wallis test (if more than two classes for comparison) or Wilcoxon rank test using R. Overall survival rate of the patients was analyzed by Kaplan-Meier method in combination with log-rank test with SPSS 20 software. The period for the survival analysis was calculated from the date of blood sampling to the recorded date of death or the last follow-up date. Differences with a P value of <0.05 were considered statistically significant.

Results

Association of SNP rs2596542 with HBV-induced HCC

In order to examine the effect of rs2596542 genotypes on the susceptibility to HBV-induced HCC, a total of 407 HCC cases and 5,657 healthy controls were genotyped. The Cochran Armitage trend test of the data revealed a nominal association

Table 1. Demographic details of subjects analyzed.

Subjects	Source	Genotyping platform	Number of Sample	Female (%)	Age (mean+/−sd)
Liver Cancer	BioBank Japan	Illumina Human Hap610-Quad	181	17.9	62.94±9.42
	University of Tokyo	Invader assay	226		
Control	BioBank Japan	Illumina Human Hap550v3	4549	47.95	55.19±12.5
	Osaka**	Illumina Human Hap550v3	934		
	University of Tokyo	Invader assay	174		
Chronic hepatitis B*	BioBank Japan	Invader assay	597	45.66	61.31±12.6
	University of Tokyo	Invader assay	102		

*Chronic hepatitis B patients without liver cirrhosis and liver cancer during enrollment.
**Healthy volunteers from Osaka Midosuji Rotary Club, Osaka, Japan.
doi:10.1371/journal.pone.0044743.t001

between HBV-induced HCC and rs2596542 in which a risk allele G was more frequent among HBV-induced HCC cases than an A allele (P = 0.029, OR = 1.19, 95% CI: 1.02–1.4; Table 2). To further investigate the effect of rs2596542 on the progression from CHB to HBV-induced HCC, we genotyped a total of 699 CHB cases without HCC. Although the progression risk from CHB to HBV-induced HCC was not statistically significant with rs2596542 (P = 0.197 by the Cochran Armitage trend test with an allelic OR = 1.3 (0.94–1.36); Table 2), we found a similar trend of association in which the frequency of a risk-allele G was higher among HBV-induced HCC patients than that of CHB subjects. Since we previously revealed that an A allele was associated with a higher risk of HCV-induced HCC with OR of 1.36 [14], the s2596542 alleles that increased the risk of HCC were opposite in HBV-induced HCC and HCV-induced HCC.

Soluble MICA levels are associated with SNP rs2596542

We subsequently performed measurement of soluble MICA (sMICA) in serum samples using the ELISA method in 176 HBV-positive HCC cases and 60 non-HBV controls. Nearly 30% of the HBV-induced HCC cases revealed the serum sMICA level of >5 pg/ml (defined as high) while the all control individuals except one showed that of ≤5 pg/ml (defined as low) ($P = 4.5 \times 10^{-6}$; Figure 1A). Then, we examined correlation between SNP rs2596542 genotypes and serum sMICA levels in HBV-positive HCC cases. Interestingly, rs2596542 genotypes were significantly associated with serum sMICA levels (P = 0.009; Figure 1B); 39% of individuals with the GG genotype and 20% of those with the AG genotype were classified as high for serum sMICA, but only 11% of those with the AA genotype were classified as high (AA+AG vs GG; P = 0.003) (Figure 1B). These findings were similar with our previous reports in which a G allele was associated with higher serum sMICA levels in HCV-induced HCC patients [14].

Negative association of variable number of tandem repeat (VNTR) with sMICA level

The *MICA* gene harbors a VNTR locus in exon 5 that consists of 4, 5, 6, or 9 repeats of GCT as well as a G nucleotide insertion into a five-repeat allele (referred as A4, A5, A6, A9, and A5.1, respectively). The insertion of G (A5.1) causes a premature translation termination and results in loss of a transmembrane domain, which may produce the shorter form of the MICA protein that is likely be secreted into serum [25]. However, the association of this VNTR locus with serum sMICA level was controversial among studies [14,26,27,28]. Therefore, we examined the association between the VNTR locus and sMICA level in HBV-induced HCC patients, and found no significant association (Figure S1 and S2), concordant with our previous report for HCV-induced HCC patients [14].

Soluble MICA levels are associated with survival of HCC patients

In order to evaluate the prognostic significance of serum sMICA levels in HCC patients, we performed survival analysis of HCC patients. A total of 111 HBV-infected HCC patients and 129 HCV-infected HCC patients were included in this analysis. The mean survival period for HBV- and HCV-infected patients with less than 5 pg/ml of serum sMICA were 67.1 months (95% CI: 61.1–73.1, n = 83), and 58.2 months (95% CI: 51.4–65.0, n = 85), respectively. On the other hand, for patients with more than 5 pg/ml of serum sMICA, the mean survival periods were 47.8 months (95% CI: 34.8–30.9, n = 28) for HBV-induced HCC patients and 59.5 months (95% CI: 51.9–67.1, n = 44) for HCV-induced HCC patients. The Kaplan-Maier analysis and log-rank test indicated that among HBV-induced HCC subjects, the patients in the high serum sMICA group showed a significantly shorter survival than those in the low serum sMICA (P = 0.008; Figure 2). In addition, we performed multi-variate analysis to test whether sMICA is an independent prognostic factor by including age and gender as covariates. The results revealed significant association of sMICA levels with overall survival (P = 0.017) but not with age and gender (Table S1).However, we found no association between the serum sMICA level and the overall survival in the HCV-induced HCC subjects (P = 0.414; Figure S3). Taken together, our findings imply the distinct roles of the *MICA* variation and sMICA between HBV- and HCV-induced hepatocellular carcinogenesis.

Vascular invasion in HBV-related HCC patients is associated with soluble MICA levels

Since sMICA levels were associated with the overall survival of HBV-related HCC patients, we tested whether sMICA levels affect survival through modulating invasive properties of tumors or size of the tumors. We tested the association between sMICA levels and vascular invasion in 35 HBV-related HCC cases, among whom 7 cases were positive and 21 cases were negative for vascular invasion. We found significant association between sMICA levels and vascular invasion (Figure 3; P = 0.014) in which 7 cases with positive vascular invasion showed high levels of sMICA (mean = 54 pg/ml) than 21 cases without vascular invasion (mean = 7.51 pg/ml). However, we found no association between tumor size and sMICA levels (P = 0.56; data not shown). These results suggest that sMICA may reduce the survival of HBV-related HCC patients by affecting the invasive properties of tumors.

Discussion

Several mechanisms such as HBV-genome integration into host chromosomal DNA [29] and effects of viral proteins including HBx [30] are shown to contribute to development and progression of HCC, while the immune cells such as NK and T cells function as key antiviral and antitumor effectors. MICA protein has been

Table 2. Association between HCC and rs2596542.

SNP	Comparison	Chr	Locus	Case MAF	Control MAF	P*	OR*	95% CI
rs2596542	HCC vs. Healthy control	6	*MICA*	0.294	0.332	0.029	1.19	1.02–1.4
rs2596542	HCC vs. CHB	6	*MICA*	0.294	0.320	0.197	1.13	0.94–1.36

Note: 407 HCC cases, 699 CHB subjects and 5,657 non-HBV controls were used in the analysis.
Chr.,chromosome; MAF, minor allele frequency; OR, odds ratio for minor allele; CI, confidence interval.
*Obtained by Armitage trend test.
doi:10.1371/journal.pone.0044743.t002

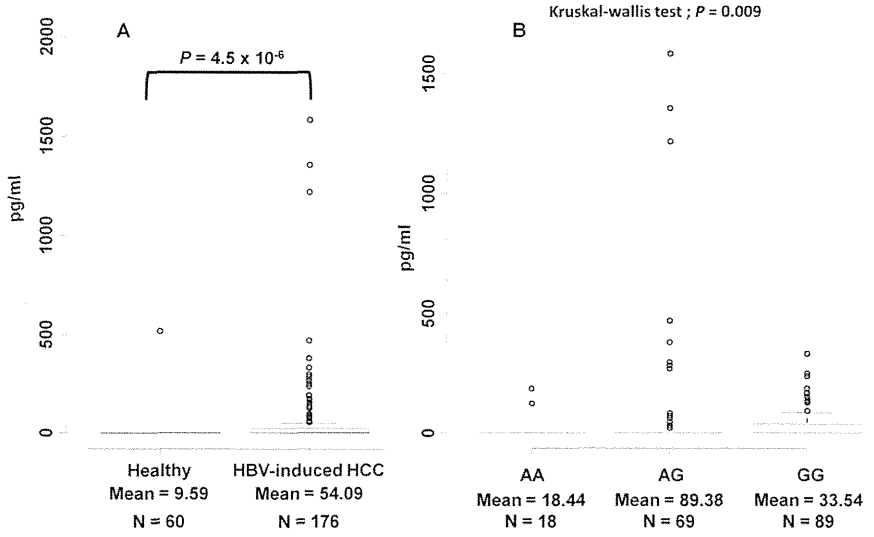

Figure 1. Soluble MICA levels are associated with HBV-related HCC. (A) Correlation between soluble MICA levels and HBV-induced HCC subjects. The y-axis displays the concentration of soluble MICA in pg/ml. The number of independent samples tested in each group is shown in the x-axis. Each group is shown as a box plot and the mean values are shown in the x-axis. The difference between two groups is tested by Wilcoxon rank test. The box plots are plotted using default settings in R. (B) Correlation between soluble MICA levels and rs2596542 genotype in HBV-positive HCC subjects. The x-axis shows the genotypes at rs2596542 and y-axis display the concentration of soluble MICA in pg/ml. Each group is shown as a box plot. $P = 0.027$ and 0.013 for AA vs. GG and AA vs. AG, respectively. The association between genotypes and sMICA levels was tested by Kruskal-wallis test, whereas the difference in the sMICA levels between AA and GG is tested by Wilcoxon rank test. The box plots are plotted using default settings in R.
doi:10.1371/journal.pone.0044743.g001

considered as a stress marker of gastrointestinal epithelial cells because of its induced expression by several external stimuli such as heat, DNA damage, and viral infections [31,32,33,34]. Here, we examined the association of rs2596542 and serum sMICA levels with HBV-induced HCC. Like in HCV-induced HCC [14], our results from ELISA revealed a significantly higher proportion

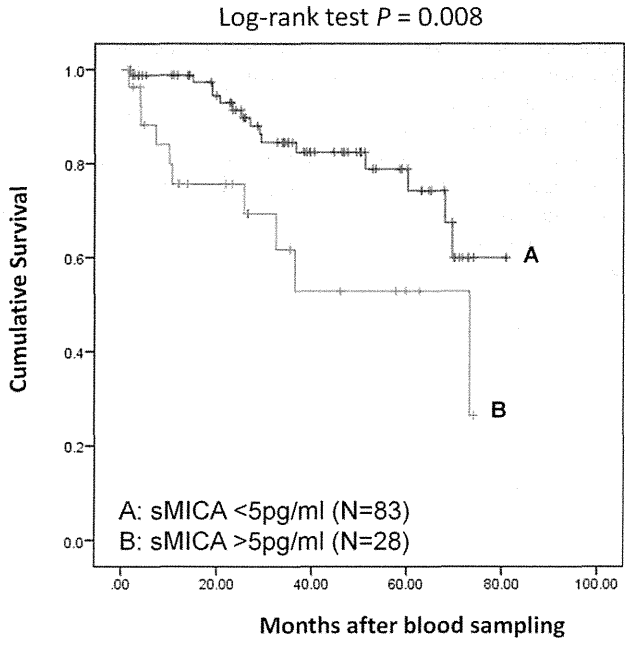

Figure 2. Kaplan-Meier curves of the patients with HBV-induced HCC. The patients were divided into two groups according to their sMICA concentration (high: >5 pg/ml and low: =<5 pg/ml). Statistical difference was analyzed by log-rank test. The y-axis shows the cumulative survival probability and x-axis display the months of the patients survival after blood sampling.
doi:10.1371/journal.pone.0044743.g002

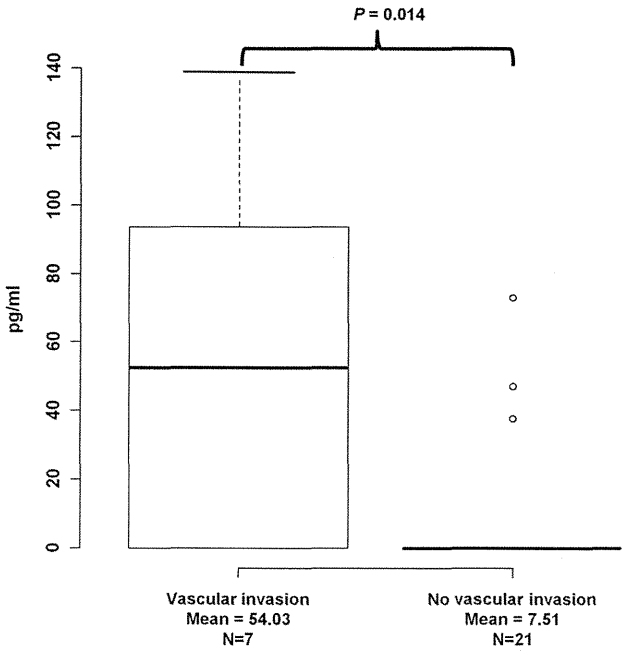

Figure 3. Correlation between soluble MICA levels and vascular invasion in HBV-induced HCC subjects. The y-axis displays the concentration of soluble MICA in pg/ml. The number of independent samples tested in each group is shown in the x-axis. Each group is shown as a box plot and the mean values are shown in the x-axis. The difference between two groups is tested by Wilcoxon rank test. The box plots are plotted using default settings in R.
doi:10.1371/journal.pone.0044743.g003

of high serum sMICA cases (nearly 30%) in the HBV-induced HCC group, compared to non-HBV individuals (1.7%). Moreover, the serum sMICA level was significantly associated with rs2596542, but not with the copy number differences of the VNTR locus, as concordant with our previous report [14].

Several studies have already indicated the roles of sMICA as prognostic markers for different types of malignant diseases [17,18,19,20]. Therefore, it is of medical importance to test whether serum sMICA levels can be used as a prognostic marker for patients with HCC. To our best knowledge, this is the first study to demonstrate the prognostic potential of sMICA for HBV-positive HCC patients; we found 19.3 months of improvement in survival among patients carrying less than 5 pg/ml of serum sMICA, compared to those having more than 5 pg/ml.

On the contrary, we found no significant correlation between sMICA levels and the prognosis of HCV-induced HCC cases. These opposite effects of *MICA* variation could be explained by the following mechanism. The individuals who carry the G allele would express high levels of membrane-bound MICA upon HCV infection and thus lead to the activation of immune cells against virus infected cells. On one hand, HBV infection results in increased expression of membrane-bound MICA as well as MMPs through viral protein HBx [35], which would result in the elevation of sMICA and the reduction of membrane-bound MICA. Since sMICA could block CD8+T cells, NK-CTL, and NK cells, higher sMICA would cause the inactivation of immune surveillance system against HBV infected cells. In other words, HBV may use this strategy to evade immune response and hence, higher levels of sMICA could be associated with lower survival rate among HBV-associated HCC. On the other hand, since HCV is not known to induce the cleavage of membrane bound MICA, individuals with low level membrane bound MICA expression (carriers of rs2596542-allele A) could be inherently susceptible for HCV-induced HCC. Thus, HBx-medicated induction of MMPs could partially explain the intriguing contradictory effect of MICA between HBV-induced HCC and HCV-induced HCC. Since we observed significant correlation of sMICA levels with vascular invasion, it may be the case that high levels of sMICA cause poor prognosis of HBV-related HCC cases by making tumors more aggressive and invasive. However it is important in future to determine the ratio of membrane-bound MICA to sMICA in case of HCV- and HBV-related HCC.

Interestingly, the immune therapy against melanoma patients induced the production of auto-antibodies against MICA [36]. Anti-MICA antibodies would exert antitumor effects through antibody-dependent cellular cytotoxicity against cells expressing membrane-bound MICA and/or activation of NK cells by inhibiting the sMICA-NKG2D interaction. However, further studies are necessary, using well-defined HBV-related HCC cohort, to investigate whether sMICA levels could be included as an additional factor to predict the survival rate among HBV-related HCC subjects. Taken together, our results indicate the potential of *MICA* variant and sMICA as prognostic biomarkers. Thus, MICA could be a useful therapeutic target for HBV-induced HCC.

Supporting Information

Figure S1 MICA repeat genotyping using capillary-based method. The alleles are annotated using GeneMapper software based on the size of the PCR product (185 bp = A4 allele, 188 bp = A5, 189 bp = A5.1, 191 bp = A6 and 200 bp = A9). The inset at the base of each peak shows the size of the PCR product with corresponding allele call by the software. The figure display all observed heterozygotes at A5.1 allele.
(TIF)

Figure S2 MICA VNTR alleles are not associated with soluble MICA levels. Each group is shown as a box plot. The difference in the sMICA values among each group is tested by Wilcoxon rank test. The box plots are plotted using default settings in R.
(TIF)

Figure S3 Kaplan-Meier curves of the patients with HCV-induced HCC. The patients were divided into two groups according to their sMICA concentration (<5 pg/ml or >5 pg/ml). Statistical difference was analyzed by log-rank test. The y-axis shows the cumulative survival probability and x-axis display the months of the patients survival after blood sampling.
(TIF)

Table S1 Clinical parameters of HBV-related HCC patients available for prognostic analyses.
(XLS)

Acknowledgments

We would like to thank all the patients and the members of the Rotary Club of Osaka-Midosuji District 2660 Rotary International in Japan, who donated their DNA for this work. We also thank Ayako Matsui and Hiroe Tagaya (the University of Tokyo), and the technical staff of the Laboratory for Genotyping Development, Center for Genomic Medicine, RIKEN for their technical support.

Author Contributions

Conceived and designed the experiments: VK KM YN. Performed the experiments: VK PHL YU HM ZD. Analyzed the data: VK PHL CT RM. Contributed reagents/materials/analysis tools: YN NK AT MK HS KT YT MS MM RT MO KK NK. Wrote the paper: VK PHL KM YN.

References

1. Kew MC (2010) Epidemiology of chronic hepatitis B virus infection, hepatocellular carcinoma, and hepatitis B virus-induced hepatocellular carcinoma. Pathol Biol (Paris) 58: 273–277.
2. Sherman M (2010) Hepatocellular carcinoma: epidemiology, surveillance, and diagnosis. Semin Liver Dis 30: 3–16.
3. Perz J, Armstrong G, Farrington L, Hutin Y, Bell B (2006) The contributions of hepatitis B virus and hepatitis C virus infections to cirrhosis and primary liver cancer worldwide. J Hepatol 45: 529–538.
4. Chen CJ, Chen DS (2002) Interaction of hepatitis B virus, chemical carcinogen, and genetic susceptibility: multistage hepatocarcinogenesis with multifactorial etiology. Hepatology 36: 1046–1049.
5. Cui R, Okada Y, Jang SG, Ku JL, Park JG, et al. (2011) Common variant in 6q26–q27 is associated with distal colon cancer in an Asian population. Gut 60: 799–805.
6. Kumar V, Matsuo K, Takahashi A, Hosono N, Tsunoda T, et al. (2011) Common variants on 14q32 and 13q12 are associated with DLBCL susceptibility. J Hum Genet England. pp. 436–439.
7. Cui R, Kamatani Y, Takahashi A, Usami M, Hosono N, et al. (2009) Functional variants in ADH1B and ALDH2 coupled with alcohol and smoking synergistically enhance esophageal cancer risk. Gastroenterology 137: 1768–1775.
8. Urabe Y, Tanikawa C, Takahashi A, Okada Y, Morizono T, et al. (2012) A genome-wide association study of nephrolithiasis in the Japanese population identifies novel susceptible loci at 5q35.3, 7p14.3 and 13q14.1. PLOS Genet 8(3): e1002541.
9. Tanikawa C, Urabe Y, Matsuo K, Kubo M, Takahashi A, et al. (2012) A genome-wide association study identifies two susceptibility loci for duodenal ulcer in the Japanese population. Nat Genet 44(4): 430–434.

10. Hata J, Matsuda K, Ninomiya T, Yonemoto K, Matsushita T, et al. (2007) Functional SNP in an Sp1-binding site of AGTRL1 gene is associated with susceptibility to brain infarction. Hum Mol Genet 16: 630–639.
11. Kamatani Y, Wattanapokayakit S, Ochi H, Kawaguchi T, Takahashi A, et al. (2009) A genome-wide association study identifies variants in the HLA-DP locus associated with chronic hepatitis B in Asians. Nat Genet 41: 591–595.
12. Mbarek H, Ochi H, Urabe Y, Kumar V, Kubo M, et al. (2011) A genome-wide association study of chronic hepatitis B identified novel risk locus in a Japanese population. Human Molecular Genetics 20: 3884–3892.
13. Zhang H, Zhai Y, Hu Z, Wu C, Qian J, et al. (2010) Genome-wide association study identifies 1p36.22 as a new susceptibility locus for hepatocellular carcinoma in chronic hepatitis B virus carriers. Nat Genet 42: 755–758.
14. Kumar V, Kato N, Urabe Y, Takahashi A, Muroyama R, et al. (2011) Genome-wide association study identifies a susceptibility locus for HCV-induced hepatocellular carcinoma. Nature genetics 43: 455–458.
15. Jinushi M, Takehara T, Tatsumi T, Kanto T, Groh V, et al. (2003) Expression and role of MICA and MICB in human hepatocellular carcinomas and their regulation by retinoic acid. Int J Cancer 104: 354–361.
16. Bauer S, Groh V, Wu J, Steinle A, Phillips JH, et al. (1999) Activation of NK cells and T cells by NKG2D, a receptor for stress-inducible MICA. Science 285: 727–729.
17. Holdenrieder S, Stieber P, Peterfi A, Nagel D, Steinle A, et al. (2006) Soluble MICA in malignant diseases. Int J Cancer 118: 684–687.
18. Nückel H, Switala M, Sellmann L, Horn PA, Dürig J, et al. (2010) The prognostic significance of soluble NKG2D ligands in B-cell chronic lymphocytic leukemia. Leukemia 24: 1152–1159.
19. Tamaki S, Sanefuzi N, Kawakami M, Aoki K, Imai Y, et al. (2008) Association between soluble MICA levels and disease stage IV oral squamous cell carcinoma in Japanese patients. Hum Immunol 69: 88–93.
20. Li K, Mandai M, Hamanishi J, Matsumura N, Suzuki A, et al. (2009) Clinical significance of the NKG2D ligands, MICA/B and ULBP2 in ovarian cancer: high expression of ULBP2 is an indicator of poor prognosis. Cancer Immunol Immunother 58: 641–652.
21. Salih H, Rammensee H, Steinle A (2002) Cutting edge: down-regulation of MICA on human tumors by proteolytic shedding. J Immunol 169: 4098–4102.
22. Groh V, Wu J, Yee C, Spies T (2002) Tumour-derived soluble MIC ligands impair expression of NKG2D and T-cell activation. Nature 419: 734–738.
23. Jinushi M, Takehara T, Tatsumi T, Hiramatsu N, Sakamori R, et al. (2005) Impairment of natural killer cell and dendritic cell functions by the soluble form of MHC class I-related chain A in advanced human hepatocellular carcinomas. J Hepatol 43: 1013–1020.
24. Nakamura Y (2007) The BioBank Japan Project. Clin Adv Hematol Oncol 5: 696–697.
25. Ota M, Katsuyama Y, Mizuki N, Ando H, Furihata K, et al. (1997) Trinucleotide repeat polymorphism within exon 5 of the MICA gene (MHC class I chain-related gene A): allele frequency data in the nine population groups Japanese, Northern Han, Hui, Uygur, Kazakhstan, Iranian, Saudi Arabian, Greek and Italian. Tissue Antigens 49: 448–454.
26. Tamaki S, Sanefuzi N, Ohgi K, Imai Y, Kawakami M, et al. (2007) An association between the MICA-A5.1 allele and an increased susceptibility to oral squamous cell carcinoma in Japanese patients. J Oral Pathol Med 36: 351–356.
27. Tamaki S, Kawakami M, Yamanaka Y, Shimomura H, Imai Y, et al. (2009) Relationship between soluble MICA and the MICA A5.1 homozygous genotype in patients with oral squamous cell carcinoma. Clin Immunol 130: 331–337.
28. Lü M, Xia B, Ge L, Li Y, Zhao J, et al. (2009) Role of major histocompatibility complex class I-related molecules A*A5.1 allele in ulcerative colitis in Chinese patients. Immunology 128: e230–236.
29. Bonilla Guerrero R, Roberts LR (2005) The role of hepatitis B virus integrations in the pathogenesis of human hepatocellular carcinoma. J Hepatol 42: 760–777.
30. Bouchard MJ, Schneider RJ (2004) The enigmatic X gene of hepatitis B virus. J Virol 78: 12725–12734.
31. Groh V, Bahram S, Bauer S, Herman A, Beauchamp M, et al. (1996) Cell stress-regulated human major histocompatibility complex class I gene expressed in gastrointestinal epithelium. Proc Natl Acad Sci U S A 93: 12445–12450.
32. Groh V, Steinle A, Bauer S, Spies T (1998) Recognition of stress-induced MHC molecules by intestinal epithelial gammadelta T cells. Science 279: 1737–1740.
33. Groh V, Rhinehart R, Randolph-Habecker J, Topp M, Riddell S, et al. (2001) Costimulation of CD8alphabeta T cells by NKG2D via engagement by MIC induced on virus-infected cells. Nat Immunol 2: 255–260.
34. Gasser S, Orsulic S, Brown EJ, Raulet DH (2005) The DNA damage pathway regulates innate immune system ligands of the NKG2D receptor. Nature 436: 1186–1190.
35. Lara-Pezzi E, Gomez-Gaviro MV, Galvez BG, Mira E, Iniguez MA, et al. (2002) The hepatitis B virus X protein promotes tumor cell invasion by inducing membrane-type matrix metalloproteinase-1 and cyclooxygenase-2 expression. J Clin Invest 110: 1831–1838.
36. Jinushi M, Hodi F, Dranoff G (2006) Therapy-induced antibodies to MHC class I chain-related protein A antagonize immune suppression and stimulate antitumor cytotoxicity. Proc Natl Acad Sci U S A 103: 9190–9195.

Microbiol Immunol 2013; 57: 122–129
doi: 10.1111/1348-0421.12011

ORIGINAL ARTICLE

Specific mutations of basal core promoter are associated with chronic liver disease in hepatitis B virus subgenotype D1 prevalent in Turkey

Mustafa Sunbul[1], Masaya Sugiyama[2], Fuat Kurbanov[3], Hakan Leblebicioglu[1], Anis Khan[3], Abeer Elkady[3], Yasuhito Tanaka[3], and Masashi Mizokami[2]

[1]Department of Infectious Diseases, School of Medicine, Ondokuz Mayis University, Kurupelit, Samsun, Turkey, [2]Department of Hepatic Diseases, The Research Center for Hepatitis and Immunology, National Center for Global Health and Medicine, Ichikawa, and [3]Department of Virology, Liver Unit, Nagoya City University Graduate School of Medical Sciences, Nagoya, Japan

ABSTRACT

The role of hepatitis B virus (HBV) genetics in the clinical manifestations of infection is being increasingly recognized. Genotype D is one of eight currently recognized major HBV genotypes. The virus is ubiquitous worldwide, but shows different features in different regions. One hundred and ninety-eight patients with chronic HBV infection were enrolled in this study, 38 of whom had been diagnosed with cirrhosis of the liver and/or hepatocellular carcinoma. HBV DNA was isolated from the patients' blood samples and the entire genome and/or the basal core promoter/core promoter region sequenced. Phylogenetic analysis of the complete genomes revealed that subgenotype D1 is the most prevalent subgenotype in Turkey, but there was no definite phylogenetic grouping according to geography for isolates from different regions within Turkey, or for isolates in Turkey relative to other parts of the world. Turkish isolates tended to be genetically similar to European and central Asian isolates. Overall, HBV-infection in Turkey appears to be characterized by early HBeAg seroconversion, a high incidence of the A1896 core promoter mutation and a small viral load. Genotype D characteristic mutations A1757 and T1764/G1766 were found in the BCP region. T1773 was associated with T1764/G1766 and a larger viral load. In conclusion, infection with HBV genotype D in Turkey has a similar clinical outcome to that of Europe and central Asia. Genotypic mutations in genotype D may be linked with disease prognosis in Turkey, but further studies with higher sample numbers and balanced clinical groups are needed to confirm this.

Key words basal core promoter, genotype D, hepatitis B virus, Turkey.

Hepatitis B virus infection is a global public health problem, affecting more than 350 million people worldwide. The clinical manifestations of this infection vary greatly and include acute self-limiting disease, an inactive carrier state and CH with progression to LC and HCC (1, 2). An accumulating body of evidence indicates that the viral genotype (3, 4) and specific mutations in the viral genome (5, 6) are important viral factors contributing to the development of HCC. The main eight genotypes of HBV (A–H) have been identified based

Correspondence
Masaya Sugiyama, Department of Hepatic Diseases, The Research Center for Hepatitis and Immunology, National Center for Global Health and Medicine, Ichikawa 272-8516, Japan.
Tel: +81 47 372 3501; fax: +81 47 375 4766; email: m.sugiyama@hospk.ncgm.go.jp

Received 3 October 2012; revised 12 November 2012; accepted 23 November 2012.

List of Abbreviations: γ-GTP, γ-glutamyl transpeptidase; AFP, alpha-fetoprotein; Alb, albumin; ALP, alkaline phosphatase; ALT, alanine transaminase; AST, aspartate aminotransferase; BCP/CP, basal core promoter/core promoter; CH, chronic hepatitis; DB, direct bilirubin; EIA, enzyme-linked immunoassay; Glob, globulin; HBeAg, hepatitis B e antigen; HBsAg, hepatitis B surface antigen; HBV, hepatitis B virus; HCC, hepatocellular carcinomas; HCV, hepatitis C virus; Kozak, Kozak sequence used in translation initiation site of eukaryotic mRNA; LC, liver cirrhosis; PLT, platelet; PT-INR, Prothrombin time-international normalized ratio; TB, total bililubin; TP, total protein.

on comparison of complete genomes, most genotypes having a distinct geographic distribution (7). There are some indications of correlations between HBV genotypes and clinical manifestations of this infection; one study showing that HBV genotype D is more strongly associated with severe liver disease and HCC than is genotype A (8). However, other studies found no association between genotype and clinical manifestations of this infection (9, 10). Specific mutations in the HBV genome reportedly affect both translation of the HBeAg and replication of HBV, thereby influencing the clinical manifestations of HBV infection and contributing to development of HCC (11, 12).

The aim of the current study was to investigate the distribution of HBV genotypes and subgenotypes in chronic hepatitis B patients in different regions of Turkey and to compare these distributions with those of HBV genotypes from other parts of the world. Our aim was to make it possible to draw inferences about disease transmission within Turkey, and between Turkey and other countries. This topic is particularly interesting, given Turkey's location at the crossroads of Europe and Asia. We also investigated the prevalence of BCP/CP mutations in patients with and without LC and/or HCC.

MATERIALS AND METHODS

Patients

In all, 198 patients with CHB were enrolled in the study. All were attendees at four clinical centers in geographically distinct parts of Turkey, namely Samsun (north), Ankara (center), Gaziantep (south) and Istanbul (west). The patients' ages ranged from 16 to 73 years. In 38 of the patients, LC or HCC had been diagnosed before enrollment (Table 1).

Diagnoses based on HBsAg seropositivity for longer than 6 months, clinical findings and liver biopsies were used to classify the patients into two clinical groups: (i) CH patients with persistently high serum ALT concentrations but no evidence of LC or HCC; and (ii) LC and/or HCC patients (hereafter referred to as LC/HCC patients) with clinical evidence of cirrhosis (e.g., coarse liver architecture, nodular liver surface and blunt liver edge) based on evidence of hypersplenism (e.g., splenomegaly demonstrated by ultrasonography or computed tomography and platelet counts of < 100,000 platelets mm^3) and complementary clinical information (e.g., ascites, jaundice, encephalopathy or esophageal varices), and/or HCC diagnosed on the basis of results of imaging studies together with high serum AFP concentrations ($\geq$ 400 ng/mL). Sera were collected from each individual and stored immediately at −70°C until use. The serological and biochemical tests were performed at Ondokuz Mayis University (Kurupelit, Turkey). Molecular analyses were performed at the Department of Virology, Liver Unit, Nagoya City, University Graduate School of Medical Science, Nagoya, Japan. The study was approved by the Ethics Committee of the School of Medicine, Ondokuz Mayis University. Informed consent was obtained from all subjects and the study was conducted in accordance with the declaration of Helsinki (as revised in Tokyo 2004).

Table 1. Summary of samples collected

City (location)	N (%)
Samsun (north)	63 (31.8)
Ankara (center)	76 (38.4)
Gaziantep (south)	20 (10.1)
Istanbul (west)	39 (19.7)
Total	198 (100)

Serological analysis

Hepatitis B surface antigen, anti-HBs, HBeAg, anti-HBe, anti-HBc IgG, anti-Delta, and anti-HCV in patient serum samples were detected by ARCHITECT (Abbott Diagnostics, Lake Forest, IL, USA). Biochemical markers, including concentrations of anti-HCV, HBeAg, TP, Alb, Glob, PT-INR, AST, ALT, γ-GTP, ALP, TB, DB, and HBV DNA and PLT counts in all samples were measured at the local hospitals.

Genotyping of hepatitis B virus

Hepatitis B surface antigen-positive samples were subjected to HBV genotyping using commercially available EIA kits (Institute of Immunology, Tokyo, Japan). This method allows discrimination among the seven major HBV genotypes (A–G) by monoclonal antibodies targeted to the pre-S2 epitopes (2). HBV genotype H was not determined in this study because the EIA kit is unable to identify it.

Sequencing and phylogenetic analysis

Nucleic acids were extracted from 100 μL of serum using a QIAamp DNA Blood Mini Kit (Qiagen, Hilden, Germany). Complete genomes were amplified using primer sets as described previously (13). Partial HBV genomes were also amplified in enhancer II/core promoter and precore regions as described previously (13).

PCR products were directly sequenced with the ABI PRISM BigDye v3.1 kit (Applied Biosystems, Foster City, CA, USA) on an ABI 3100 DNA automated sequencer. All sequences were analyzed in both forward and reverse directions. Complete and partial genomes were assembled